Geoderma Regional 10 (2017) 48–63

Contents lists available at ScienceDirect

Geoderma Regional

journal homepage: www.elsevier.com/locate/geodrs

Geochemical fingerprinting of volcanic soils used for wetland rice in West Sumatra, Indonesia

Dian Fiantis[a,*], Gusnidar[a], Brendan Malone[b], Robert Pallasser[b], Eric Van Ranst[c], Budiman Minasny[b]

[a] Department of Soil Science, Faculty of Agriculture, Universitas Andalas, Kampus Limau Manis, Padang 25163, Indonesia
[b] Sydney Institute of Agriculture, The University of Sydney, 1 Central Avenue, Australian Technology Park, Eveleigh, NSW 2015, Australia
[c] Department of Geology (WE13), Faculty of Sciences, Ghent University, Campus Sterre S8, Krijgslaan 281, B-9000 Gent, Belgium

ARTICLE INFO

Keywords:
Weathering indices
Discriminant analysis
Soil carbon fractions
X-ray fluorescence
Andisols

ABSTRACT

Cultivation of paddy (rice) in volcanic soils is commonly practiced in West Sumatra, Indonesia. This study aims to provide a detailed geochemical fingerprinting of topsoils of paddy fields derived from volcanic materials in the vicinity of mountain (Mt) Marapi, Mt. Sago, Mt. Singgalang, Mt. Tandikek and Caldera Maninjau in West Sumatra, Indonesia as a function of different geochronology of volcanic parent materials. Seventy-nine topsoil samples were collected along an altitudinal gradient ranging from 44 m in the Maninjau area to 1220 m above sea level (a.s.l.) at Mt. Singgalang. In addition to conventional physical and chemical analysis, geochemical analysis was carried out using a portable X-ray fluorescent spectrometer (XRF) and organic matter composition was analyzed using mid-infrared Fourier transform infrared spectroscopy (FTIR). The chemical composition of the volcanic paddy soils in this area is controlled by the origin of parent materials and weathering processes. Soils of Mt. Sago have lower soil pH (5.46) and smaller cation exchange capacity (CEC = 16.5 $cmol_c\ kg^{-1}$) compared to soils from the other three mountains. On the other hand, soils of Mt. Marapi have higher pH (6.05) and larger CEC (19.8 $cmol_c\ kg^{-1}$). Linear discriminant analysis revealed that the major geochemical elements in volcanic paddy soils can be ascribed to the different volcanic origin. The results of Mahalanobis distance statistics clearly separated soils of Mt. Sago with the other four soils. Soils from Mt. Marapi were also dissimilar with the other three soils, while soils from Mt. Singgalang-Tandikek and Maninjau were more related. Clear differentiation among weathering indices was also observed. Soils of Mt. Sago again showed higher weathering stages when evaluated using indices with immobile elements (Al_2O_3, Fe_2O_3, TiO_2 and Zr). The following sequence of the degree of weathering can be concluded: Sago > Maninjau > Marapi > Singgalang-Tandikek. Soil analysis using FTIR revealed that labile aliphatic (C—H) compounds were the dominant organic matter fractions in these soils with abundances between 64 and 77%. Soils with total C less than 2% tend to be dominated by aromatic fractions, while soils greater than 2% C are dominated by the more labile aliphatic fractions. In conclusion, although the soils have been cultivated with paddy for hundreds of years, they still retain distinct geochemical signatures that can be revealed using a portable XRF.

1. Introduction

Volcanic soils are quite unique in terms of their physical, chemical and morphological properties (Ugolini and Dahlgren, 2002). Soils derived from volcanic ash are known to be fertile and are one of the most productive soils in the world. They are also known to have a high human carrying capacity, as evidenced by dense population in areas near volcanoes (Small and Naumann, 2001). Mohr (1938) compared population densities for different districts near Mount Merapi, Central Java, and found higher population densities in areas with soils derived from volcanic ash. Paddy cultivation in Indonesia is often found in areas near volcanoes (Winkler et al., 2016). This is in contrast with most paddy-growing areas in Asia, which are in lowlands with soils originated from alluvial and colluvial deposits in Thailand (Prakongkep et al., 2008), marine sediments in Zhejiang Province China (Kölbl et al., 2014), sedimentary deposits in both Mekong delta of Vietnam (Kontgis et al., 2015) and Northwest Cambodia (Nguyen et al., 2013), on recent alluvial and deltaic sediments in the Ganges and Meghna floodplains in Bangladesh (Martin et al., 2015), and sulfidic materials in coastal areas of Peninsular Malaysia (Aimrun et al., 2004).

* Corresponding author.
E-mail address: dianfiantis@faperta.unand.ac.id (D. Fiantis).

http://dx.doi.org/10.1016/j.geodrs.2017.04.004
Received 9 November 2016; Accepted 3 April 2017
Available online 29 April 2017
2352-0094/

Paddy cultivation on soils derived from volcanic parent material is commonly found along the Barisan Mountain Ranges of Sumatra Indonesia. These mountain ranges are a volcanic arc over a length of about 1700 km, and the site of 11 active volcanoes (Hochstein and Sudarman, 1993). These active volcanoes often eject solid volcanic materials to the atmosphere which eventually descend on the Earth's surface. The history of volcanic eruptions in Sumatra can be traced back to the super-eruption of Toba some 74,000 years ago (Smyth et al., 2011) and to very recent eruptions of Mt. Sinabung (Anda and Sukarman, 2016). Both of these volcanoes are situated in North Sumatra. The deposition of these tephra materials alters the geochemical properties of the volcanic soils.

West Sumatra is strongly influenced by volcanic activity, covering an area of about 6202 km^2. In this region, there are 4 active volcanoes (considered as type A) namely Mt. Marapi, Mt. Tandikek, Mt. Talang and Mt. Kerinci, 3 dormant (type B) volcanoes being Mt. Sago, Mt. Singgalang and Mt. Talamau, and then the extinct Mt. Maninjau (referred to as Maninjau Caldera). The differences in their volcanic activity ultimately result in differing degrees of soil weathering, soil formation, and soil geochemical characteristics. These volcanic regions are well-known to be fertile and are the central agricultural production both for horticulture and grains crops. The present work focuses on volcanic paddy soils in West Sumatra and investigated the influence of geochronology on soil geochemical elements, weathering pattern and organic matter composition. We hypothesized that differences exist between nutrient potential reserve and their availability in the topsoils of the various volcanic paddy soils.

2. Materials and methods

2.1. Regional setting, geology and soil information of studied sites

The studied sites are situated in volcanic areas in West Sumatra with a total area about 3028 km^2 covering Mt. Marapi, Tandikek, Singgalang and Sago and Maninjau caldera. Seventy-nine volcanic paddy-soil samples were taken from the top layer (0 to 20 cm) from various locations spread over the central part of West Sumatra, Indonesia (Fig. 1A). The location for this volcanic region is enclosed by the geographic coordinates 99° 55′ 12″ to 100° 50′ 35″ E and 0° 01′ 29″ to 0° 42′ 10.15″ S. We chose soils developed from volcanic ash along an altitudinal gradient ranging from 44 m in Maninjau area to 1220 m above sea level (a.s.l.) in Mt. Singgalang. They were located at three transects on slopes with west (W), east (E), south (S), north (N), south east (SE), south west (SW), north east (NE) exposure at Mt. Marapi, Mt. Sago and Maninjau. Mt. Singgalang and Mt. Tandikek are named as two separate peaks but are geologically two parts of one volcano, i.e. the north facing slope being Mt. Tandikek and the south facing slope being Mt. Singgalang.

Volcano eruptions occurred at 52 ± 3 ka in Maninjau with an estimated volume of 220–250 km^3 of silicic or rhyolitic tephra which covered the surrounding region (Alloway et al., 2004), with an estimated area up to 1420 km^2 (Leo et al., 1980). The silicic deposits of Maninjau tuff were found at various locations, such as at a depth of 373 m beneath the andesitic tephra bed of Mt. Marapi in Desa Melintang some 36 km eastward from the eruptive source, 30 km south at a depth of 180 m below the andesitic tephra bed of Tandikek, and 15 km north with a thickness of 60 m underlying the 0.24 m of andesitic tephra of Mt. Singgalang (Alloway et al., 2004). The last eruption of Mt. Tandikek was in 1924 (Van Bemmelen, 1949), and Mt. Talang in 2005 (Fiantis et al., 2011), located 95.6 km southeast of Mt. Marapi. Mt. Marapi is still active and erupted volcanic ash on November 15, 2015 (Muslim, 2015). No record of volcanic eruption has occurred from Mt. Sago or Mt. Singgalang since 1600 (Van Bemmelen, 1949). Paddy cultivation in volcanic ash soils of West Sumatra extends from a few meters above sea level to altitudes of > 1500 m at Mt. Marapi. These topographic conditions of paddy soils, from lowland to sloping terraces of highland areas offer a unique opportunity to study geochronosequences of volcanic ash soils.

The Maninjau volcanic center shows multiple paroxysmal events. At least three of such events took place, at 50 ka, 70 ka and 80 ka (Nishimura, 1980). These eruptions blasted welded and unwelded pumiceous tuff of Maninjau and the unwelded materials were blown up to 50 km to the east, 75 km to the southeast and extending 20 km westward to the coastline (Alloway et al., 2004). The geological map of studied area is shown in Fig. 1B. There were three different morphologies of volcanic materials from Maninjau; (1) Quaternary pumice tuff (Qpt) are the older deposit, white in colour, pumiceous rhyolite tuff formed extensive exposures to 30 km west of Maninjau caldera to coastal line and those deposited at 20 to 40 km distance to the north are tuff of pumice flow and basalto-andesitic lithics with little mafic constituents. The pyroclastic flow consists of glass shards with up to 80% pumice and lithic fraction. The lithics occur as flow breccia, several meters thick, intercalated among the pumice tuff; (2) Quaternary hypersthene pumice tuff (Qhpt) are the beige, semi-consolidated, yellow- to brown-weathering pumice fragments and contain approximately 10% phenocrysts of labradorite, hornblende, augite and hypersthene on the southeast side of Maninjau. Localities in the east of Maninjau are deposits overlying a darker, scoriaceous lapilli tuff of Mt. Marapi. The same materials were also deposited on the southeast, over a 50-km elongated depression between Maninjau and the Singgalang-Tandikat volcano couple. The colour of the volcanic materials is white to yellowish grey when fresh, weathering into deep rusty brown, consisting of hornblende-hypersthene pumice tuff, with predominant lapilli 2 to 10 cm in diameter, and (3) Quaternary Maninjau (Qmaj) is the next oldest sequence and are pyroclastic flows with andesitic composition found surrounding the caldera (Leo et al., 1980, Kastowo et al., 1996).

Andesites of Mt. Marapi are regarded as relatively young volcanic rocks since Mt. Marapi is still active. The volcanic rocks consist of andesitic to basaltic breccia and lava boulders. The andesites of Singgalang-Tandikek are considered intermediate in age between the andesites of Mt. Marapi and the Maninjau caldera, and comprise undifferentiated lava flows, lahars and tuffs (Kastowo et al., 1996). The igneous rocks of Mt. Sago comprise andesitic to basaltic breccia, agglomerate, scoriaceous lava fragments, lahar deposits and lava (Silitonga and Kastowo, 1995).

The soils are classified according to Soil Survey Staff (2014) as Hydrudands (Andisols) which occupy an area of about 120,200 ha, Hapludands (Andisols) at about 135,700 ha, Humudepts (Inceptisols) with an area 12,470 ha, Dystrudepts (Inceptisols) 139,000 ha and Hapludults (Ultisols) coverage is 1647 ha. Mean annual temperature across sites ranges from 18 to 26 °C and average annual precipitation ranges from 2500 to 4500 mm $year^{-1}$. Higher amounts of precipitation are common on the western side of Maninjau, Mt. Singgalang-Tandikek and Mt. Sago. The eastern slope of Mt. Marapi and Mt. Sago is drier than the western slopes, but the eastern part of Mt. Singgalang-Tandikek has similar precipitation as the western part of Mt. Marapi.

2.2. Soil sampling and analysis

A purposive sampling design was adopted in this study considering the restricted budget and vast areas to be covered (up to 3202.8 km^2 of the volcanic areas of Mts. Marapi, Singgalang, Tandikek, Sago and Maninjau). About 20% of this volcanic area is presently cultivated with paddy on flat or plateau, undulating to sloping areas. Paddy fields on terraces are commonly found in the hilly and mountainous volcanic regions. At each selected site of paddy field, undisturbed and disturbed soil samples were collected at the depth 0 to 20 cm. At all sites, samples were taken after rice harvesting, under field-moist condition. Undisturbed soil samples were obtained using standard ring sampler with a known volume to determine the soil's bulk density. At each site, five soil samples were taken in an orthogonal pattern and composited

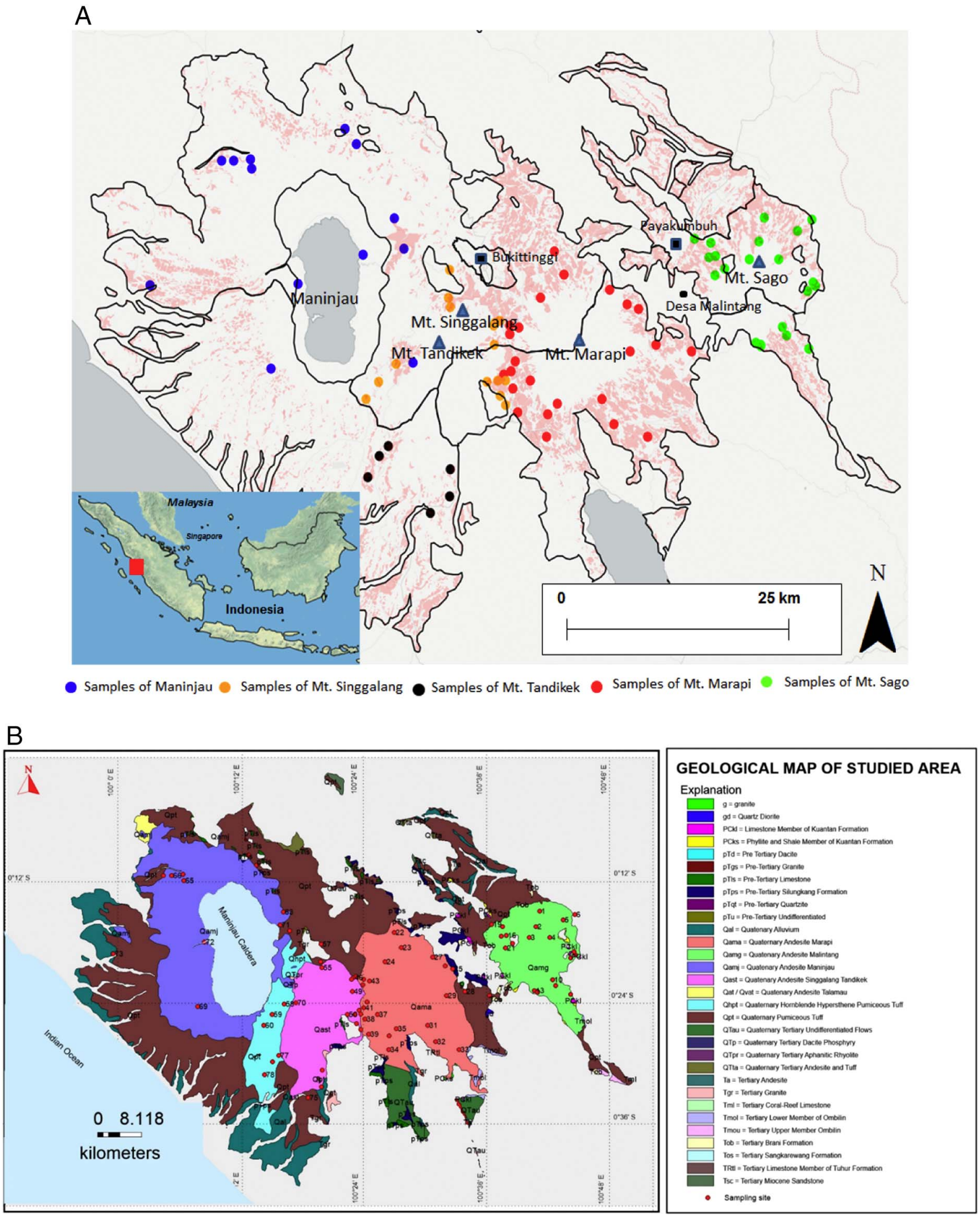

Fig. 1. A. Location of sampling sites in the volcanic region of West Sumatra.B. Geological map of studied area.

into one sampling unit. The samples were then brought to the laboratory, air-dried, homogenised by grinding and sieved to a size fraction smaller than 2 mm.

Soil pH was measured in H_2O and 1 M KCl at a solution ratio of 1:5 after 30 min of equilibration. The available phosphate anion was analysed colorimetrically using a visible-light spectrophotometer with the Bray 1 method and the potential P or total inorganic P was analysed by using HCl 25% extraction (Tan, 2005). The P retention was determined with the method described by Blakemore et al. (1987). Exchangeable cations and cation exchange capacity (CEC) were determined by 1 N NH_4OAc, pH 7.0 extraction; the leachate was used to determine the exchangeable base cations, which were measured using the atomic absorption spectrophotometry (AAS). Percent base saturation (BS) is the percentage of the CEC occupied by the basic cations. Saturation of individual base cations was calculated by dividing the content of individual exchangeable cation by effective CEC and then expressed as a percentage (Anda, 2012). The total carbon (TC) and total nitrogen (TN) content of the soil samples were determined by dry combustion with a Vario max CNS Elemental Analyzer (Elementar Analysensysteme GmbH, Hanau, Germany).

Table 1
Paddy soil characteristics developed from volcanic parent materials.

A.

No	Volcano	Slope direction	Elevation	Easting	Southing	Sand	Silt	Clay	BD	pH H_2O	pH KCl	ΔpH
						%			Mg m^{-3}			
1	Sago	North	600	687,805	9,972,177	9	20	71	1.04	5.56	3.56	− 2.00
2	Sago	North	800	687,149	9,969,351	11	17	72	0.64	5.32	3.43	− 1.89
3	Sago	North	1022	685,909	9,967,349	14	29	57	0.58	5.39	3.76	− 1.63
4	Sago	North East	879	689,712	9,967,345	10	22	68	0.81	5.14	3.59	− 1.55
5	Sago	North East	570	692,125	9,970,601	9	16	75	0.96	5.81	4.11	− 1.70
6	Sago	North East	504	694,299	9,971,522	12	25	63	0.65	6.18	4.24	− 1.94
7	Sago	East	725	693,468	9,963,686	20	22	59	0.84	5.58	3.54	− 2.04
8	Sago	East	650	694,370	9,964,273	7	18	74	0.84	4.84	3.35	− 1.49
9	Sago	East	640	694,106	9,964,761	8	20	72	0.92	5.20	4.33	− 0.87
10	Sago	South East	970	690,238	9,959,686	23	14	63	1.06	5.06	3.36	− 1.70
11	Sago	South East	810	690,728	9,958,667	9	40	50	0.98	5.62	3.74	− 1.88
12	Sago	South East	628	693,522	9,957,054	8	11	82	0.85	5.24	3.26	− 1.98
13	Sago	South	999	686,824	9,957,708	18	30	52	0.66	6.09	4.13	− 1.96
14	Sago	South	952	687,453	9,957,536	17	39	44	0.61	5.23	3.75	− 1.48
15	Sago	South	939	687,436	9,957,439	51	28	21	0.80	5.35	3.39	− 1.96
16	Sago	West	745	681,744	9,967,721	10	25	65	0.90	6.10	4.46	− 1.64
17	Sago	West	916	682,863	9,966,321	12	18	69	0.90	5.21	3.40	− 1.81
18	Sago	West	610	681,062	9,969,314	11	21	68	0.86	5.55	3.73	− 1.82
19	Sago	North West	544	679,007	9,969,730	8	14	77	0.70	5.09	3.20	− 1.89
20	Sago	North West	686	680,816	9,967,614	13	13	74	0.91	5.37	3.68	− 1.69
21	Sago	North West	884	681,607	9,965,485	14	29	57	0.69	5.70	4.09	− 1.61
22	Marapi	North	898	661,237	9,968,265	39	33	28	0.95	5.90	3.83	− 2.07
23	Marapi	North	1067	662,529	9,965,568	16	40	44	0.89	5.51	3.81	− 1.70
24	Marapi	North	1219	659,505	9,962,955	27	42	31	0.66	5.95	4.01	− 1.94
25	Marapi	North East	978	671,944	9,961,672	22	25	53	0.56	6.13	4.18	− 1.95
26	Marapi	North East	1052	670,540	9,962,222	19	49	32	0.65	5.41	4.04	− 1.37
27	Marapi	North East	1134	668,258	9,963,832	38	34	28	0.65	6.45	4.45	− 2.00
28	Marapi	East	810	674,148	9,957,565	18	39	42	0.92	6.18	4.13	− 2.05
29	Marapi	East	1011	670,790	9,956,776	43	15	42	0.97	5.95	4.15	− 1.80
30	Marapi	East	595	678,634	9,956,787	10	22	68	0.78	5.38	3.32	− 2.06
31	Marapi		970	667,300	9,951,403	17	31	52	0.81	5.60	3.86	− 1.74
32	Marapi	South East	725	668,764	9,948,453	16	37	47	1.05	6.75	3.65	− 3.10
33	Marapi	South East	575	673,062	9,947,028	14	32	54	1.05	6.83	4.76	− 2.07
34	Marapi	South	685	660,216	9,947,015	28	56	16	0.89	6.07	4.35	− 1.72
35	Marapi	South	1020	661,612	9,950,829	46	38	16	0.90	6.08	4.52	− 1.56
36	Marapi	South	805	658,130	9,953,412	47	32	21	0.66	5.55	4.38	− 1.17
37	Marapi	South West	1188	655,859	9,952,590	47	40	13	0.85	6.57	4.99	− 1.58
38	Marapi	South West	1000	655,859	9,952,590	34	53	13	0.84	6.10	4.38	− 1.72
39	Marapi	South West	848	656,579	9,949,834	37	53	10	0.70	5.94	4.51	− 1.43
40	Marapi	West	1015	654,829	9,954,126	35	44	22	0.75	6.25	4.65	− 1.60
41	Marapi	West	1051	655,645	9,954,605	44	33	23	0.91	6.75	4.76	− 1.99
42	Marapi	West	1142	656,282	9,955,661	54	33	13	1.15	6.45	4.59	− 1.86
43	Marapi	North West	1149	656,713	9,959,506	37	37	26	0.85	6.13	4.39	− 1.74
44	Marapi	North West	1120	655,519	9,958,785	59	29	12	0.62	5.39	4.26	− 1.13
45	Marapi	North West	1097	655,609	9,959,767	46	37	17	1.12	5.86	4.05	− 1.81
46	Singgalang-Tandikek	North East	1062	653,711	9,960,099	36	26	38	0.82	6.00	4.09	− 1.91
47	Singgalang-Tandikek	North East	1106	653,435	9,959,801	26	40	35	0.55	6.13	4.32	− 1.81
48	Singgalang-Tandikek	North East	1043	654,252	9,960,280	32	46	22	0.82	6.05	4.59	− 1.46
49	Singgalang-Tandikek	East	1061	653,571	9,957,569	35	40	25	0.74	5.89	3.91	− 1.98
50	Singgalang-Tandikek	East	1009	652,649	9,953,374	28	48	24	0.75	5.69	4.10	− 1.59
51	Singgalang-Tandikek	East	983	655,065	9,952,390	25	43	31	0.82	6.09	4.13	− 1.96
52	Singgalang-Tandikek	South East	1076	655,065	9,953,508	38	39	23	0.98	5.75	3.72	− 2.03
53	Singgalang-Tandikek	South East	973	654,323	9,951,730	40	47	13	0.81	6.34	4.69	− 1.65
54	Singgalang-Tandikek	South East	886	655,071	9,950,689	27	46	28	0.80	5.98	4.23	− 1.75
55	Singgalang-Tandikek	North	1220	647,969	9,961,900	41	27	31	1.01	5.91	3.71	− 2.20
56	Singgalang-Tandikek	North	1102	647,735	9,962,981	39	8	53	0.71	5.28	3.45	− 1.83
57	Singgalang-Tandikek	North	958	647,842	9,966,164	20	38	42	1.07	6.75	4.63	− 2.12
58	Singgalang-Tandikek	West	785	641,082	9,955,296	22	56	23	0.45	5.70	4.33	− 1.37
59	Singgalang-Tandikek	West	663	638,860	9,953,376	50	21	28	0.45	5.71	4.24	− 1.47
60	Singgalang-Tandikek	West	552	637,373	9,951,408	54	31	16	0.46	5.36	4.24	− 1.12
61	Maninjau	North	661	636,078	9,980,530	19	39	43	0.54	5.77	3.04	− 2.73
62	Maninjau	North	531	634,624	9,982,320	22	33	45	0.86	5.95	3.65	− 2.30
63	Maninjau	North East	1028	640,937	9,972,011	20	41	39	0.58	5.64	3.54	− 2.10
64	Maninjau	North East	1043	642,068	9,968,617	36	34	30	0.73	5.89	3.77	− 2.12
65	Maninjau	North West	730	622,752	9,977,749	20	46	34	0.58	5.06	3.12	− 1.94
66	Maninjau	North West	490	620,536	9,978,633	24	51	25	0.96	5.21	3.40	− 1.81
67	Maninjau	North West	400	618,984	9,978,633	24	37	39	0.97	5.98	3.71	− 2.27
68	Maninjau	South West	430	622,616	9,978,978	32	33	35	nd	6.35	4.58	− 1.77
69	Maninjau	South West	457	625,238	9,954,827	56	8	35	0.96	5.75	4.30	− 1.45
70	Maninjau	East	987	643,260	9,955,548	40	36	24	nd	5.35	3.62	− 1.73

(continued on next page)

Table 1 *(continued)*

A.

No	Volcano	Slope direction	Elevation	Easting	Southing	Sand %	Silt	Clay	BD $Mg\ m^{-3}$	pH H_2O	pH KCl	ΔpH
71	Maninjau	East	479	634,908	9,971,130	42	32	26	nd	5.24	3.30	− 1.94
72	Maninjau	West	173	628,690	9,964,553	26	36	37	0.71	6.02	4.18	− 1.84
73	Maninjau	West	44	609,795	9,964,407	40	50	10	0.48	5.88	4.39	− 1.49
74	Singgalang-Tandikek	South	153	647,904	9,940,230	41	45	14	0.50	6.09	4.66	− 1.43
75	Singgalang-Tandikek	South	122	645,433	9,938,296	32	38	30	0.68	5.33	3.32	− 2.01
76	Singgalang-Tandikek	South	299	648,037	9,943,274	55	34	11	0.43	5.37	4.48	− 0.89
77	Singgalang-Tandikek	South West	262	640,080	9,945,978	43	43	14	0.30	5.38	4.28	− 1.10
78	Singgalang-Tandikek	South West	145	637,488	9,942,434	28	57	15	0.71	5.74	4.18	− 1.56
79	Singgalang-Tandikek	South West	199	638,998	9,944,848	53	34	13	0.68	5.81	4.58	− 1.23

No	Volcano	Org C %	N	C/N	Avai. P $mg\ kg^{-1}$	P-Pot $mg\ kg^{-1}$	P Ret.	CEC ($cmol\ kg^{-1}$)	Exc. Ca	Exc. Mg	Exc. K	Exc. Na	BS %
1	Sago	3.94	0.29	13.59	5.51	93.90	92	16.04	4.19	2.96	0.77	1.38	58
2	Sago	3.06	0.28	10.94	6.85	98.72	93	12.57	4.45	2.60	0.64	1.15	70
3	Sago	5.27	0.50	10.55	12.77	77.58	98	19.51	3.48	2.50	0.62	1.08	39
4	Sago	4.64	0.28	16.57	5.38	104.30	96	22.11	4.29	2.20	0.84	0.87	37
5	Sago	3.49	0.29	12.03	0.09	57.32	90	10.84	4.55	2.11	0.93	1.27	82
6	Sago	3.34	0.29	11.53	3.18	49.97	88	17.34	4.77	2.70	0.65	1.17	54
7	Sago	4.24	0.15	28.28	3.34	109.73	93	15.18	4.65	2.90	0.72	1.19	62
8	Sago	4.00	0.33	12.12	6.95	116.43	92	14.31	5.87	2.27	0.55	1.36	70
9	Sago	3.45	0.29	11.91	4.47	103.83	92	14.74	5.16	2.50	0.63	0.87	62
10	Sago	3.15	0.31	10.16	6.20	138.75	95	16.91	4.97	1.91	0.70	0.76	49
11	Sago	4.12	0.22	18.73	1.30	98.82	94	13.44	5.32	2.76	0.64	0.81	71
12	Sago	4.14	0.35	11.84	13.61	117.49	93	15.61	5.45	2.27	0.98	1.12	63
13	Sago	7.01	0.52	13.49	10.17	125.51	99	20.38	6.23	2.11	0.73	1.04	50
14	Sago	5.39	0.35	15.40	21.11	102.28	97	18.21	5.77	2.50	0.62	0.87	54
15	Sago	3.48	0.23	15.14	18.25	97.48	94	13.88	5.68	2.20	0.52	1.31	70
16	Sago	2.99	0.26	11.48	4.26	49.92	99	19.08	5.55	2.44	0.61	1.12	51
17	Sago	4.47	0.35	12.77	9.63	106.88	94	15.61	6.23	2.34	0.58	0.59	62
18	Sago	4.81	0.39	12.33	2.80	117.97	98	18.21	5.23	3.03	0.66	0.85	54
19	Sago	3.68	0.35	10.51	5.13	84.05	93	15.18	4.87	2.53	0.51	1.04	59
20	Sago	3.40	0.35	9.70	26.76	144.57	93	16.48	4.16	2.44	0.72	1.15	51
21	Sago	5.69	0.45	12.65	1.16	156.07	99	21.25	4.52	2.86	0.67	1.02	43
22	Marapi	2.73	0.20	13.67	2.81	44.53	90	15.61	4.32	1.97	0.74	1.25	53
23	Marapi	3.30	0.31	10.65	0.09	81.04	100	22.11	4.03	2.24	0.68	0.89	35
24	Marapi	3.69	0.32	11.54	1.78	47.80	96	18.21	3.74	2.04	0.65	1.06	41
25	Marapi	4.33	0.31	13.96	5.52	76.86	99	19.51	4.48	2.27	0.70	0.93	43
26	Marapi	5.50	0.50	11.00	9.10	136.80	100	19.51	4.87	2.63	0.84	1.25	49
27	Marapi	3.33	0.36	9.24	1.93	95.25	99	20.38	4.00	2.53	0.89	1.19	42
28	Marapi	3.33	0.32	10.41	3.60	48.75	94	16.48	4.36	2.83	0.62	0.98	53
29	Marapi	3.55	0.28	12.67	1.43	107.67	98	18.64	4.07	2.60	0.68	1.06	45
30	Marapi	3.16	0.31	10.19	3.12	62.08	94	22.11	4.65	2.27	0.72	1.36	41
31	Marapi	2.82	0.36	7.83	1.62	75.97	96	22.11	5.00	2.11	0.88	1.06	41
32	Marapi	2.66	0.26	10.23	0.81	38.81	90	21.25	5.19	2.50	1.00	1.21	47
33	Marapi	1.21	0.15	8.06	2.50	40.83	90	21.68	4.81	2.90	0.86	1.02	44
34	Marapi	3.09	0.25	12.37	9.52	78.97	92	21.68	5.52	2.24	0.73	0.89	43
35	Marapi	4.66	0.38	12.27	1.02	79.73	99	18.21	5.84	2.50	0.81	1.25	57
36	Marapi	3.27	0.73	4.48	12.08	73.10	92	18.64	6.10	2.20	0.83	1.17	55
37	Marapi	3.42	0.32	10.70	0.23	70.66	100	16.04	5.42	2.34	0.93	1.04	61
38	Marapi	4.35	0.38	11.44	12.78	205.51	97	24.28	5.23	2.53	1.00	0.91	40
39	Marapi	3.54	0.46	7.70	9.49	246.20	99	23.85	6.10	2.30	0.66	0.81	41
40	Marapi	3.11	0.23	13.53	31.66	141.10	93	21.25	5.42	2.44	0.94	0.98	46
41	Marapi	1.94	0.19	10.20	10.84	44.61	90	21.25	5.32	2.83	0.96	1.12	48
42	Marapi	1.64	0.22	7.43	99.07	229.60	91	17.78	5.19	2.90	0.87	1.00	56
43	Marapi	3.21	0.31	10.35	3.88	139.73	98	21.68	4.81	2.57	0.72	0.95	42
44	Marapi	2.64	0.25	10.58	15.80	38.50	91	14.31	4.13	2.50	0.83	1.06	60
45	Marapi	2.54	0.25	10.16	68.43	283.17	93	18.21	3.94	2.86	0.89	1.12	48
46	Singgalang-Tandikek	5.21	0.26	20.04	3.50	89.73	98	26.02	4.81	2.93	0.93	1.21	38
47	Singgalang-Tandikek	2.85	0.26	10.95	7.08	85.72	95	22.55	5.19	2.01	0.82	1.23	41
48	Singgalang-Tandikek	3.60	0.23	15.66	2.07	107.32	97	19.51	4.65	2.11	0.91	0.87	44
49	Singgalang-Tandikek	3.17	0.31	10.23	12.92	147.87	96	18.64	5.58	2.50	1.00	1.08	55
50	Singgalang-Tandikek	3.41	0.33	10.33	2.94	85.08	95	18.64	5.74	1.91	1.04	1.27	53
51	Singgalang-Tandikek	3.59	0.36	9.98	21.20	175.72	96	21.68	5.52	1.84	1.11	1.34	45
52	Singgalang-Tandikek	3.41	0.32	10.67	62.70	291.28	97	16.91	6.13	2.34	1.17	1.23	64
53	Singgalang-Tandikek	4.23	0.47	9.00	9.43	302.99	99	21.25	5.77	2.27	0.99	0.87	47
54	Singgalang-Tandikek	3.51	0.36	9.76	11.90	242.84	98	20.38	4.52	2.20	1.05	0.98	43
55	Singgalang-Tandikek	3.36	0.25	13.43	7.90	156.87	96	19.08	3.94	2.44	0.98	1.02	44

(continued on next page)

Table 1 *(continued)*

No	Volcano	Org C %	N	C/N	Avai. P mg kg^{-1}	P-Pot mg kg^{-1}	P Ret.	CEC (cmol kg^{-1})	Exc. Ca	Exc. Mg	Exc. K	Exc. Na	BS %
56	Singgalang-Tandikek	2.37	0.25	9.49	10.84	102.29	95	16.91	4.32	2.70	1.04	0.74	52
57	Singgalang-Tandikek	2.35	0.23	10.22	0.67	81.66	95	21.25	3.87	2.86	0.98	0.85	40
58	Singgalang-Tandikek	6.50	0.38	17.10	2.14	71.97	97	16.91	5.23	2.27	1.02	0.61	54
59	Singgalang-Tandikek	7.30	0.51	14.31	1.47	108.81	99	15.18	4.81	2.57	1.16	1.25	64
60	Singgalang-Tandikek	6.83	0.41	16.66	14.16	82.33	92	12.57	5.77	2.34	1.04	1.10	82
61	Maninjau	3.08	0.39	7.90	2.35	43.51	90	14.74	5.19	2.90	0.77	1.17	68
62	Maninjau	1.56	0.25	6.22	0.58	26.14	90	13.44	4.77	2.27	0.70	1.25	67
63	Maninjau	3.70	0.31	11.95	11.72	138.19	97	23.41	4.48	1.65	0.65	1.06	33
64	Maninjau	3.87	0.35	11.06	4.57	124.53	97	19.08	4.32	2.01	0.84	0.93	42
65	Maninjau	4.07	0.28	14.54	7.42	50.05	90	15.61	5.58	2.50	0.93	0.98	64
66	Maninjau	3.70	0.25	14.80	6.58	70.07	92	13.01	5.42	1.94	0.88	1.02	71
67	Maninjau	1.93	0.15	12.86	1.06	37.24	91	17.34	5.10	2.17	0.73	1.08	52
68	Maninjau	3.21	0.44	7.29	0.87	122.41	100	22.11	4.65	2.40	0.65	1.15	40
69	Maninjau	3.68	0.22	16.71	0.46	84.13	97	19.08	3.74	2.67	0.76	0.89	42
70	Maninjau	2.08	0.25	8.34	36.52	68.55	88	14.31	4.32	2.27	0.83	1.27	61
71	Maninjau	3.55	0.26	13.66	17.14	33.06	87	16.91	5.52	2.86	0.79	1.06	60
72	Maninjau	4.67	0.36	12.96	14.33	135.35	95	19.51	4.81	2.57	0.73	1.17	48
73	Maninjau	7.66	0.36	21.29	0.71	126.12	99	23.41	4.26	2.17	0.62	1.08	35
74	Singgalang-Tandikek	7.66	0.52	14.73	0.66	131.66	100	16.04	4.61	1.91	0.65	0.95	51
75	Singgalang-Tandikek	3.24	0.22	14.71	6.74	19.62	90	13.88	4.23	2.27	0.70	1.27	61
76	Singgalang-Tandikek	7.61	0.42	18.12	21.01	123.69	99	14.74	3.84	2.20	0.59	1.34	54
77	Singgalang-Tandikek	12.68	0.83	15.28	30.32	185.40	99	21.25	4.84	1.97	0.764-103	1.08	41
78	Singgalang-Tandikek	4.19	0.38	11.04	6.59	81.92	96	21.68	5.29	2.86	0.963-077	0.93	46
79	Singgalang-Tandikek	7.03	0.54	13.01	3.97	125.50	97	19.08	4.58	2.60	0.826-667	1.04	47

No	Volcano	Si_o (%)	Al_o	Fe_o	$Al_o + 1/2Fe_o$
1	Sago	0.60	1.29	0.49	2.10
2	Sago	0.64	0.94	0.53	1.83
3	Sago	0.57	1.22	0.61	2.24
4	Sago	0.57	1.22	0.74	2.46
5	Sago	0.43	1.47	0.65	2.55
6	Sago	0.48	1.26	1.20	3.26
7	Sago	0.48	1.36	0.80	2.69
8	Sago	0.56	1.08	0.93	2.64
9	Sago	0.61	0.92	1.09	2.74
10	Sago	0.53	1.02	0.56	1.96
11	Sago	0.48	1.28	0.79	2.61
12	Sago	0.52	1.37	0.90	2.86
13	Sago	0.57	1.30	0.75	2.55
14	Sago	0.49	0.94	0.81	2.29
15	Sago	0.40	1.15	0.59	2.13
16	Sago	0.63	1.14	0.81	2.49
17	Sago	0.59	1.25	0.98	2.89
18	Sago	0.49	1.54	0.83	2.92
19	Sago	0.52	1.73	0.78	3.04
20	Sago	0.54	1.32	0.75	2.57
21	Sago	0.51	1.00	0.85	2.42
22	Marapi	0.58	0.86	0.86	2.29
23	Marapi	0.47	1.18	0.80	2.51
24	Marapi	0.47	1.25	0.98	2.87
25	Marapi	0.52	1.51	0.92	3.04
26	Marapi	0.58	1.77	1.01	3.46
27	Marapi	0.59	2.36	1.24	4.43
28	Marapi	0.48	1.31	0.92	2.84
29	Marapi	0.27	1.48	1.10	3.32
30	Marapi	0.39	1.51	0.87	2.96
31	Marapi	0.22	1.78	1.10	3.61
32	Marapi	0.53	0.81	0.82	2.17
33	Marapi	0.37	0.99	0.72	2.19
34	Marapi	0.45	1.24	0.88	2.70
35	Marapi	0.55	1.54	1.00	3.21
36	Marapi	0.60	1.37	1.07	3.15
37	Marapi	0.51	2.00	0.75	3.24
38	Marapi	0.25	2.04	0.60	3.04
39	Marapi	0.31	2.46	0.71	3.65

(continued on next page)

Table 1 *(continued)*

No	Volcano	Si_o	Al_o	Fe_o	$Al_o + 1/2Fe_o$
		(%)			
40	Marapi	0.58	1.95	0.83	3.33
41	Marapi	0.57	1.95	0.67	3.06
42	Marapi	0.50	1.30	0.76	2.56
43	Marapi	0.59	2.08	0.67	3.19
44	Marapi	0.58	2.24	0.79	3.56
45	Marapi	0.62	1.19	0.79	2.51
46	Singgalang-Tandikek	0.28	1.30	0.79	2.61
47	Singgalang-Tandikek	0.42	0.75	0.63	1.80
48	Singgalang-Tandikek	0.50	0.93	0.58	1.90
49	Singgalang-Tandikek	0.30	0.97	0.66	2.08
50	Singgalang-Tandikek	0.26	1.48	0.46	2.24
51	Singgalang-Tandikek	0.59	2.11	0.67	3.22
52	Singgalang-Tandikek	0.30	2.11	0.64	3.17
53	Singgalang-Tandikek	0.34	1.43	0.76	2.69
54	Singgalang-Tandikek	0.29	1.66	0.69	2.82
55	Singgalang-Tandikek	0.52	2.46	0.61	3.49
56	Singgalang-Tandikek	0.53	1.73	0.76	2.99
57	Singgalang-Tandikek	0.63	1.56	0.91	3.08
58	Singgalang-Tandikek	0.68	1.38	1.08	3.18
59	Singgalang-Tandikek	0.54	1.38	0.96	2.99
60	Singgalang-Tandikek	0.25	2.14	0.79	3.45
61	Maninjau	0.24	2.08	1.30	4.25
62	Maninjau	0.18	1.94	1.06	3.70
63	Maninjau	1.17	2.11	1.05	3.86
64	Maninjau	0.71	1.54	0.80	2.87
65	Maninjau	0.44	1.71	0.79	3.04
66	Maninjau	0.48	1.91	0.87	3.35
67	Maninjau	0.43	1.29	1.00	2.97
68	Maninjau	0.44	1.69	1.07	3.47
69	Maninjau	0.47	0.95	0.91	2.46
70	Maninjau	0.26	0.96	0.53	1.83
71	Maninjau	0.29	1.03	0.57	1.99
72	Maninjau	0.28	1.65	0.58	2.62
73	Maninjau	0.31	1.90	0.49	2.72
74	Singgalang-Tandikek	0.34	1.46	0.55	2.37
75	Singgalang-Tandikek	0.29	2.06	0.64	3.13
76	Singgalang-Tandikek	0.33	2.80	0.81	4.16
77	Singgalang-Tandikek	0.28	2.99	0.99	4.63
78	Singgalang-Tandikek	0.29	1.79	0.59	2.77
79	Singgalang-Tandikek	0.27	1.63	0.77	2.92

B.

Variables	Units	Mean values ± Std Dev							
		Maninjau (n = 13)		Singgalang-Tandikek (n = 21)		Marapi (n = 24)		Sago (n = 21)	
pH H_2O		5.70 ± 0.38	bc	5.83 ± 0.37	ab	6.05 ± 0.55	a	5.46 ± 0.36	c
pH KCl		3.74 ± 0.49	b	4.18 ± 0.39	a	4.25 ± 0.39	a	3.72 ± 0.37	b
Bulk density	$Mg\ m^{-3}$	0.74 ± 0.19	ab	0.69 ± 0.21	ab	0.84 ± 0.16	a	0.82 ± 0.37	a
P retention	%	93.62 ± 3.23	b	96.68 ± 4.30	a	95.32 ± 3.65	ab	94.66 ± 3.22	ab
Available P	%	8.02 ± 10.25	a	11.44 ± 14.07	a	17.34 ± 13.13	a	8.13 ± 7.27	a
Potential P (HCl 25%)	$mg\ kg^{-1}$	81.45 ±	b	133.35 ± 42.56	a	103.64 ± 72.28	ab	102.46 ± 70.75	ab
Exch. Ca	$cmol_c\ kg^{-1}$	4.78 ± 0.56	a	4.92 ± 0.68	a	4.86 ± 0.69	a	5.02 ± 0.73	a
Exch. Mg	$cmol_c\ kg^{-1}$	2.34 ± 0.36	a	2.34 ± 0.33	a	2.46 ± 0.27	a	2.48 ± 0.31	a
Exch. K	$cmol_c\ kg^{-1}$	0.76 ± 0.09	bc	0.94 ± 0.16	a	0.81 ± 0.12	b	0.68 ± 0.12	c
Exch. Na	$cmol_c\ kg^{-1}$	1.09 ± 0.12	a	1.065 ± 0.20	a	1.06 ± 0.14	a	1.05 ± 0.21	a
Sum of cations	$cmol_c\ kg^{-1}$	8.96 ± 0.79	a	9.25 ± 0.81	a	9.19 ± 0.79	a	9.23 ± 0.65	a
CEC	$cmol_c\ kg^{-1}$	17.84 ± 3.62	ab	18.77 ± 3.28	a	19.78 ± 2.61	a	16.52 ± 2.90	b
Base saturation	%	52 ± 13.31	ab	51 ± 10.42	b	47 ± 6.91	b	57 ± 11.34	a
Ca saturation	%	53.29 ± 4.02	a	52.98 ± 4.02	a	52.65 ± 5.13	a	54.18 ± 3.21	a
Mg saturation	%	26.05 ± 3.03	a	25.39 ± 3.57	a	26.89 ± 3.79	a	27.00 ± 3.23	a
K saturation	%	8.50 ± 1.01	b	10.13 ± 0.99	a	8.81 ± 1.37	b	7.42 ± 1.49	c
Total C	%	2.99 ± 1.05	ab	3.34 ± 1.35	a	2.42 ± 0.69	b	3.12 ± 0.90	ab
Total N	%	0.30 ± 0.11	a	0.36 ± 0.16	a	0.32 ± 0.24	a	0.34 ± 0.18	a
C/N		9.98 ± 0.72	ab	9.31 ± 0.62	ab	8.89 ± 2.24	b	9.74 ± 1.30	a

Soil mid-infrared spectra were acquired using a Bruker Tensor 37 DRIFTS spectrometer (Bruker Optics, Ettlingen, Germany) fitted with an HTS-XT microplate/detector module. Soil subsamples were firmly packed into the microplate wells and uniformly levelled where one of the wells was designated for the KBr reference. The infrared beam was produced from a Globar source and the beam-splitter was a KBr crystal. The mercury-cadmium-telluride (MCT) detector built into the HTS-XT module was liquid-N_2 cooled. Spectra were recorded in the range 4000–600 cm^{-1} with a sampling resolution of 4 cm^{-1} and collecting 60 scans per spectrum (averaged) using the Bruker OPUS 6.5 software (Bruker Optics, Ettlingen, Germany). Spectral analysis was performed using spectroscopy package with R-Studio (Campbell et al., 2016).

Elemental concentration of volcanic paddy-soil samples was determined using an XL3T 955 portable X-ray fluorescence (Thermo Fisher Scientific, Tewksbury, Ma 01876 USA) for a total period of 120 s with 3 replications in each sample. The XRF was used in the laboratory in a bench-top accessory stand (with the nose pointing upwards) and was connected to a computer via USB. The XRF was used in the mining mode of the standard factory calibration. For the integrity of measurement, we monitored the precision of the XRF via standard certified reference materials prior to analysing the soil materials and after every 15 samples. The specific standard reference materials used were: National Institute of Standards and Technology (NIST) 2709a – San Joaquin Soil, USGS geochemical reference material 180-673 USGS SAR-M, and Blank SiO_2 (99.995%) reference material (180-647). We did not note any instrument drift throughout the measurement procedure. Samples were placed in a series of plastic containers, with a circular polypropylene ® X-Ray film (TF-240-2510), 63.5 mm in diameter and 4 µm (0.16 mil) thickness. The lower orifice of the container was covered with the polypropylene film and, with the help of two rings of the same material, a taut wrinkle-free sample support window was created. The container was then filled with soil materials through the upper orifice, gently pressed to obtain a compact sample, and closed with a lid.

2.3. Chemical weathering indices

Weathering indices were calculated from elemental concentrations. Several indices are used in this study:

1. Ruxton weathering index: $R = SiO_2/Al_2O_3$ as proposed by Ruxton (1968) that relates silica loss to total element loss of alumina, as alumina is considered to be immobile during weathering. The scale ranges from 0 to 10, with 0 as fully weathered and 10 for fresh materials (Fiantis et al., 2010).
2. Desilication index (DI) = $SiO_2/(Fe_2O_3 + Al_2O_3 + TiO_2)$, is a molar ratio of mobile silica to three resistant or less mobile oxides of Fe, Al and Ti. Weathering of silicate minerals and downward leaching of the silica and bases results in enrichment of less mobile elements Al, Fe and Ti (Singh et al., 1998; Stockmann et al., 2016). Small values of Ruxton, and DI indicated high weathering, while large values indicate least weathering.
3. Ba/Sr leaching = Ba/Sr, both Ba and Sr are an earth-alkali elements with different leaching behaviour, Sr is more soluble than Ba. This index was introduced by Nesbitt et al. (1980), best suited to carbonate free material (Buggle et al., 2011) and useful to detect the weathering processes in silicate minerals such as plagioclase, pyroxene, amphibole and biotite (Nesbitt et al., 1980). Large values indicate intense leaching.
4. Bases loss = $Al_2O_3/(CaO + MgO + K_2O)$, utilises the differences in soil chemical composition of the immobile element of alumina over three mobile elements. It was slightly modified from the formula used by Kronberg and Nesbitt (1981). This formula indicates the enrichment of alumina and the loss of mobile elements during weathering process, with large values indicating a high base loss.
5. Elemental ratio of elements resistant to weathering = Ti/Zr, both Ti and Zr are considered as immobile or resistant elements (Stockmann et al., 2016)
6. Calcium to titanium ratio (CTR) = CaO/TiO_2, this index uses a ratio of a mobile element of CaO to the immobile element of TiO_2 (Bétard, 2012).

2.4. Geochemical data analysis

Discriminant analysis was applied in this study to explain the variance structure of the geochemical properties of volcanic paddy soils. The measured variables were analysed in the JMP Pro 11 software. Linear discriminant analysis is a multivariate analysis tool that finds combinations of sets of geochemical variables that best separate the parent materials. Discriminant analysis has been used in soils of North America (Drew et al., 2010), European volcanic soil studies (Martínez-Cortizas et al., 2007), Azores archipelago (Parelho et al., 2014), paddy soils originating from USA and Asia (Rinklebe et al., 2016). It is also used to correlate between the ages and chemical composition of volcanic ashes in Western USA (Ward et al., 1993). Linear discriminant analysis derived canonical variables, which are linear combinations of the geochemical variables that summarise between-class variation, similar to principal component analysis. The first canonical variate has the highest possible multiple correlations with the groups. Details of discriminant analysis in soil survey and classification can be found in Webster (1977).

2.5. FTIR data analysis

Demyan et al. (2012) proposed the use of specific absorbance peaks of mid-infrared spectra to characterize soil organic matter and related functional groups. They further established four distinct peaks in the mid-infrared region and hypothesized the stability of each organic functional group, i.e. (1) peak at 2930 cm^{-1} is the integration limited by spectral bands 3010–2800 cm^{-1} associated with vibrations of aliphatic C—H stretching and considered as labile carbon fraction; (2) peak at 1620 cm^{-1} is the integration limited by spectral bands 1660–1580 cm^{-1} from aromatic compound with C═C and/or —COO^- stretching assumed as carbon with intermediate stability; (3) peak at 1530 cm^{-1} is the integration limited by spectral region 1546–1520 cm^{-1} of other aromatic C═C stretching bands with intermediate stability; (4) peak at 1159 cm^{-1} is the integration limit from spectral C—O bonds of poly-alcoholic and ether groups with unknown stability status. For each of the peaks, a numerical integration was calculated from its upper and lower boundaries with a local baseline to obtain the peak area. Following Demyan et al. (2012), the relative abundance for each of the carbon (functional) groups was expressed as the ratio of the area of each peak over the sum of the four peak areas.

3. Results and discussion

3.1. General soil properties

As can be seen in Table 1A and B, the paddy soils studied here presented some differences in chemical parameters depending on their parent materials. Although paddy soils' solution reaction became neutral under water saturation, the soil pH tends to decrease when the paddy fields are drained prior to harvest. Overall the soils were characterised by strongly acidic to neutral pH (in H_2O) ranging from 4.84 to 6.82 and soil pH (in KCl) ranging from 3.04 to 4.99, with paddy soils of Mt. Marapi having higher pH values than those of Mt. Singgalang-Tandikek, Maninjau, and Sago. The pH-KCl values were consistently less than those measured in H_2O, with ΔpH values range from −0.89 to −3 indicating soils with overall negative surface charge.

The average values of soil bulk density met the criteria for andic soil properties (< 0.90 Mg m^{-3}) with higher values found in Mt. Marapi

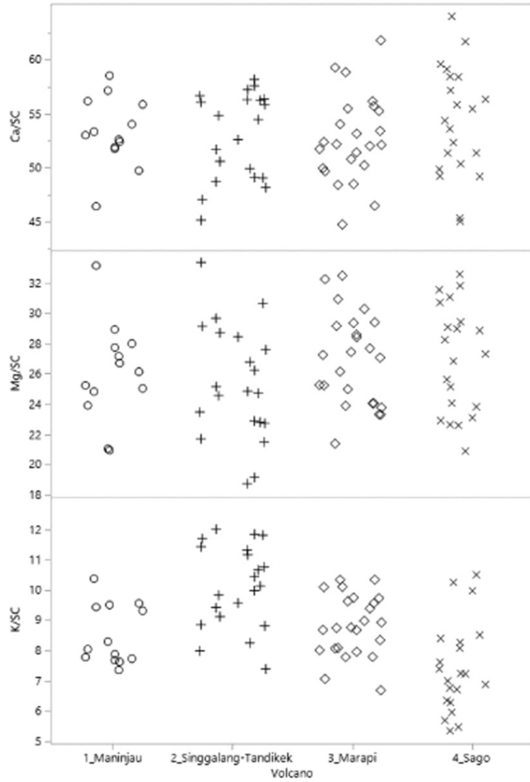

Level	Number	Mean	Std Dev	Lower 95%	Upper 95%
Maninjau	13	53.29	3.21	51.35	55.23
Singgalang-Tandikek	21	52.97	4.02	51.15	54.81
Marapi	24	52.64	4.02	50.95	54.34
Sago	21	54.18	5.13	51.85	56.52

Level	Number	Mean	Std Dev	Lower 95%	Upper 95%
Maninjau	13	26.05	3.23	24.10	28.00
Singgalang-Tandikek	21	25.39	3.79	23.67	27.12
Marapi	24	26.89	3.03	25.61	28.17
Sago	21	26.99	3.57	25.37	28.63

Level	Number	Mean	Std Dev	Lower 95%	Upper 95%
Maninjau	13	8.50	0.99	7.9072	9.098
Singgalang-Tandikek	21	10.13	1.37	9.5029	10.750
Marapi	24	8.81	1.01	8.3815	9.237
Sago	21	7.42	1.49	6.7455	8.101

Fig. 2. Visualization of the entire cation saturation using scatter plot matrix and their statistical data.

compared to Sago, Maninjau, and Singgalang-Tandikek. From this result, it can be assumed that there is no effect of paddy cultivation, which involves artificial submergence and drainage, ploughing and puddling, to the soils' bulk density. Thus, volcanic paddy soils from West Sumatra still retain low bulk density, which reflects the porous structure, easy root penetration, and high drainage, and high water holding capacity.

These soils have a relatively high total C content (2 to 6.5%), with the highest total carbon, total nitrogen, C/N ratio and sum of base cations observed in soils of Mt. Singgalang-Tandikek, followed by soils of Mt. Sago, Maninjau, and Marapi. The total nitrogen values in the studied soils were similar and rated as high (Hazelton and Murphy, 2007). The C/N ratio values ranged from 3.1 to 14.68, with increasing trend in the order of Marapi, Sago, Singgalang-Tandikek and Maninjau. Overall, the mean values of C/N ratio in all samples were < 10 indicating an optimum rate of organic matter decomposition in the studied soils. Comparable C/N values were previously reported for non-paddy volcanic soils along the southern slope of Marapi (Fiantis, 2000). In that study, it was showed that the soil's C/N ratio is relatively stable after 20 years of anthropogenic disturbance via paddy cultivation.

The available P in all soils is considered low to moderate; the highest value found in Mt. Marapi and shows a decreasing trend in Mt.

Table 2
Elemental oxides composition and weathering indices.

Variables	Units	Mean values ± Std Dev							
		Maninjau		Singgalang-Tandikek		Marapi		Sago	
SiO_2	%	31.41 ± 4.93	bc	34.27 ± 6.59	b	38.78 ± 6.71	a	29.04 ± 4.14	c
Al_2O_3	%	12.20 ± 2.44	b	9.73 ± 2.69	c	12.58 ± 2.73	b	15.62 ± 0.74	a
CaO	%	0.67 ± 0.36	b	1.34 ± 0.37	a	1.55 ± 0.71	a	0.29 ± 0.18	c
MgO	%	0.51 ± 0.22	a	0.44 ± 0.21	ab	0.50 ± 0.29	a	0.34 ± 0.21	b
K_2O	%	0.40 ± 0.28	b	0.59 ± 0.15	a	0.57 ± 0.19	a	0.20 ± 0.12	c
SO_3	%	0.62 ± 0.13	c	0.98 ± 0.21	a	0.77 ± 0.27	b	0.35 ± 0.12	d
P_2O_5	mg kg^{-1}	2318 ± 1391	b	3773 ± 1893	a	4515 ± 2656	a	2568 ± 787	b
Fe_2O_3	%	7.31 ± 2.17	b	5.27 ± 1.76	c	7.31 ± 2.36	b	9.04 ± 2.15	a
Zr	mg kg^{-1}	210.53 ± 36.94	b	172.38 ± 37.64	c	213.55 ± 34.77	b	302.63 ± 22.54	a
Sr	mg kg^{-1}	69.1 ± 52.32	c	131.62 ± 35.90	b	164.95 ± 61.34	a	45.94 ± 33.43	c
Ti	mg kg^{-1}	4451 ± 951	c	3650 ± 970	d	5270 ± 1222	b	6162 ± 528	a
Ba	mg kg^{-1}	213.06 ± 94.01	b	195.93 ± 82.56	b	244.25 ± 87.81	b	332.38 ± 72.79	a
Ti/Zr	Mean	21.33 ± 4.29	b	21.06 ± 2.88	b	24.51 ± 2.75	a	20.46 ± 2.24	b
SiO_2/Al_2O_3	Mean	2.70 ± 0.83	c	3.67 ± 0.68	a	3.23 ± 0.97	b	1.87 ± 0.31	d
Desilication	Mean	1.67 ± 0.64	b	2.30 ± 0.49	a	1.99 ± 0.68	ab	1.151 ± 0.25	c
Ba/Sr leaching	Mean	4.50 ± 3.81	b	1.47 ± 0.80	c	1.80 ± 1.17	c	9.36 ± 4.34	a
Base loss	Mean	9.42 ± 5.44	b	4.24 ± 1.34	b	6.04 ± 3.94	b	23.91 ± 13.88	a
Sesquioxide ratio	Mean	1.733 ± 0.665	b	2.391 ± 0.511	a	2.075 ± 0.711	ab	1.200 ± 0.257	c
CaO/TiO_2	Mean	0.0987 ± 0.066	b	0.2363 ± 0018	a	0.1993 ± 0.0169	a	0.0292 ± 0.019	c

Table 3
Correlations among elemental oxides composition.

Parameters	SiO_2	Al_2O_3	CaO	MgO	K_2O	SO_3	P_2O_5	Fe_2O_3	Zr	Ti
SiO_2	1	0.077	0.545	0.175	0.658	0.192	0.227	− 0.422	0.060	− 0.220
Al_2O_3	0.077	1	− 0.284	0.253	− 0.253	− 0.235	0.099	0.547	0.702	0.701
CaO	0.545	− 0.284	1	0.278	0.671	0.619	0.439	− 0.470	− 0.402	− 0.510
MgO	0.175	0.253	0.278	1	0.241	0.189	0.168	− 0.068	− 0.045	− 0.005
K_2O	0.658	− 0.253	0.671	0.241	1	0.400	0.345	− 0.544	− 0.236	− 0.518
SO_3	0.192	− 0.235	0.619	0.189	0.400	1	0.686	− 0.474	− 0.346	− 0.447
P_2O_5	0.227	0.099	0.439	0.168	0.345	0.686	1	− 0.251	− 0.077	− 0.256
Fe_2O_3	− 0.422	0.547	− 0.470	− 0.068	− 0.544	− 0.474	− 0.251	1	0.573	0.742
Zr	0.060	0.702	− 0.402	− 0.045	− 0.236	− 0.346	− 0.077	0.573	1	0.737
Ti	− 0.220	0.701	− 0.510	− 0.005	− 0.518	− 0.447	− 0.256	0.742	0.737	1

Singgalang-Tandikek, Maninjau, and Sago, respectively. It is common to find low available P in volcanic soils as these soils are well known to have a high capacity to retain phosphate. The P retention was found between 88 and 99% and all of the values met the andic soil properties requirement ≥ 85%. A previous study in 1996 showed that available P was also low for non-paddy volcanic soils along southern toposequence of Mt. Marapi and it decreased as P retention and sorption increased (Fiantis, 2000), suggested that there is no change after 20 years of cultivation.

The CEC values of the studied soils were rated as low to moderate (10.84 to 26.02 $cmol_c\ kg^{-1}$) with an average value of 18.56 $cmol_c\ kg^{-1}$. The lowest values were found in paddy soils of Mt. Sago (average 16.5 $cmol_c\ kg^{-1}$) which are significantly lower than those of Maninjau and Mt. Singgalang-Tandikek, while CEC of soils from Mt. Marapi is the highest (average 19.8 $cmol_c\ kg^{-1}$). The present CEC data of soils of Mt. Marapi were less than those reported by Fiantis et al. (2002) for arable volcanic soils on the southern slope of Mt. Marapi. These lower values were presumably due to intensive cultivation of soils compared to uncultivated samples of the same soil types. Comparable results were published by Fauzi and Stoops (2004) that CEC values of volcanic ash soils from West Java in the range of 15.3–27 $cmol_c\ kg^{-1}$ and from 14.3 to 19.6 $cmol_c\ kg^{-1}$ for volcanic soils of Mt. Merapi from Central Java (Anda, 2012) and finally 29–59 $cmol_c\ kg^{-1}$ for those from Dieng volcanic complex of Central Java (Van Ranst et al., 2008).

The magnitude of exchangeable K showed differences between each group of soils, the highest value obtained in soils originated from Mt. Singgalang-Tandikek, followed by Marapi, Maninjau and Sago. On the other hand, the exchangeable Ca, Mg and Na were similar in all soils. The proportion of each base cation on the exchange complex can be related to plant requirements. The exchange complex ideally should be saturated with 65% Ca, 10% Mg and 5% K for optimum plant growth (Kopittke and Menzies, 2007). The average Ca saturation values are as follows: Mt. Sago (54% Ca), Maninjau and Singgalang-Tandikek (53% Ca) and Marapi (52% Ca) as shown in Fig. 2. The level of Mg saturation ranged from 18% in soils of Maninjau to 32% in soils of Mt. Sago and furthermore the average value was higher in soils at Mt. Sago and Marapi (27% Mg), followed by Maninjau (26% Mg), and Singgalang-Tandikek (25% Mg). The lowest K saturation was in soils of Mt. Sago (5% K) and the highest was in Mt. Singgalang-Tandikek (12% K) which was significantly higher than in Mt. Sago (4.26% K), Mt. Marapi (4.16% K) or in Maninjau. The K saturation in soils of Marapi and Maninjau were very similar but significantly different to Sago. This implies all studied soils have cation imbalance for Ca which was < 20% of the ideal saturation at 65%, while both K and Mg saturation met the requirement. This is similar to the finding of Anda (2012) for volcanic soils of Mt. Merapi in Central Java that were extremely saturated with Mg, high Ca saturation but K was less than expected. This cation imbalance rating may need revision for tropical volcanic soils.

The average base saturation values of all soils were considered as moderate, with the lowest value in soils of Mt. Marapi (47%) and the highest in Mt. Sago (57%). From the chemical analysis for all 4 soils, Mt. Sago soils showed unique (the most extreme) characteristics of having the lowest pH, CEC, and base saturation. The opposite occurs in soils from Mt. Marapi which showed the highest pH, CEC, and base saturation. Soils from Maninjau and Singgalang-Tandikek are intermediate between these two extremes.

3.2. Geochemical signatures of paddy soils

All of the paddy soil samples were developed from volcanic parent materials with rhyolitic to andesitic-basaltic composition from various deposition times. Although the soil has been used as paddy fields for hundreds of years, soils developed from different volcanic materials have unique geochemical characteristics. The major elemental concentration is presented in Table 2 and the relationships among them in Table 3. Total silica (SiO_2) is between 29 and 39%, which means they are moderately weathered when compared to fresh ash samples which are around 50–60% (Fiantis et al., 2011). The silica content in paddy soils of Mt. Sago were significantly lower than those in Maninjau, Singgalang-Tandikek, and Marapi, suggesting that the loss in silica was high in Mt. Sago. On the other hand, the Al_2O_3, Fe_2O_3, and TiO_2

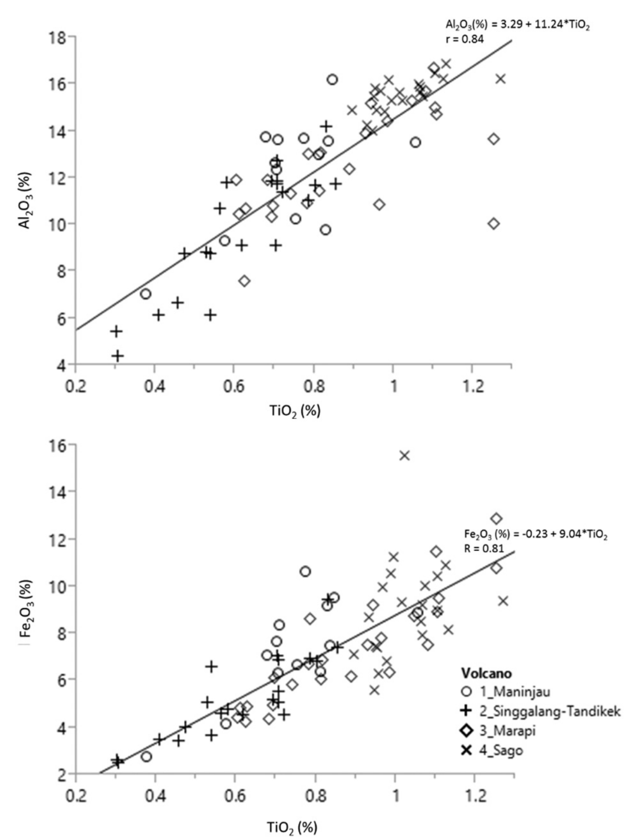

Fig. 3. Bivariate fit of total Al_2O_3 and Fe_2O_3 by TiO_2.

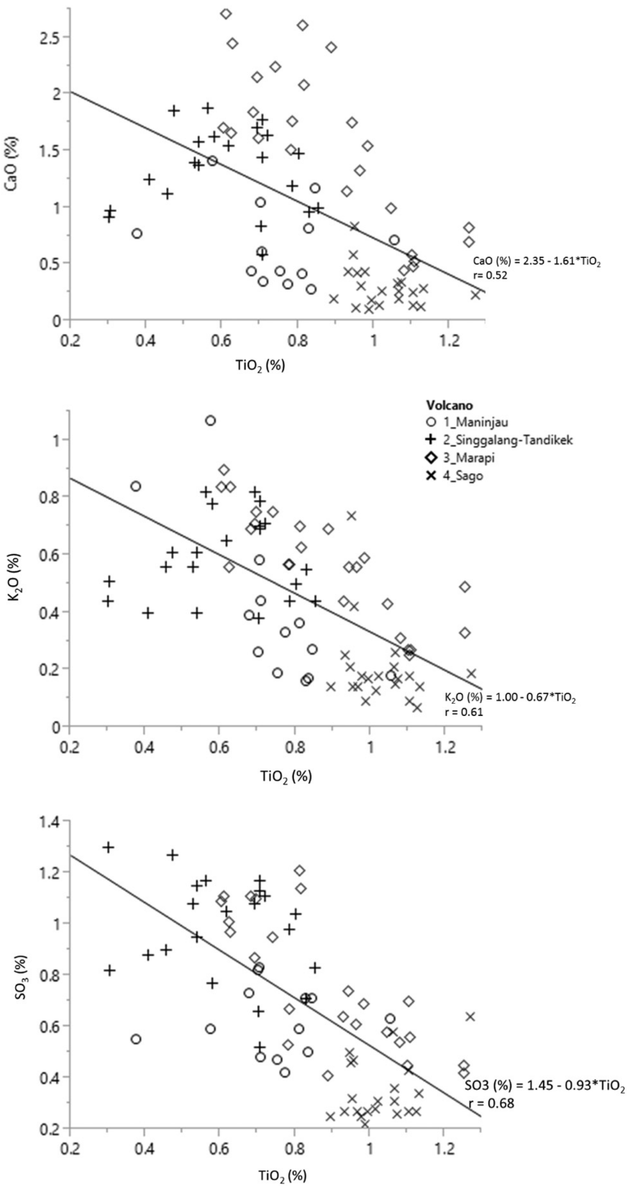

Fig. 4. Bivariate fit of total CaO, K_2O and SO_3 by TiO_2.

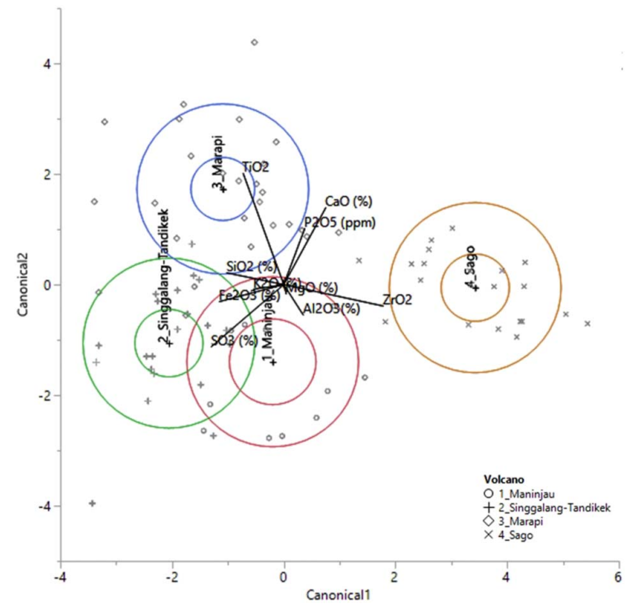

Fig. 5. Plot of canonical discriminant functions for separating volcanic paddy soils from different parent materials.

contents are higher in paddy soils of Mt. Sago, compared to those in Maninjau, Marapi and Singgalang-Tandikek. These oxides are considered as the least mobile species as such greater amounts are expected to be found in more weathered soils. This is also reflected in concentrations of Al_2O_3, and Fe_2O_3 which increase with increasing TiO_2 (Fig. 3). The bases oxide content (CaO, MgO, and K_2O) are significantly less in Mt. Sago and the highest concentration are found in Mt. Marapi and Singgalang-Tandikek. Concentrations of CaO, K_2O and SO_3 display a strong negative correlation with TiO_2 (r = 0.52–0.68) as shown in Fig. 4. The depleted contents on these mobile base cations implied they were leached during pedogenesis resulting in enriched TiO_2. Hence, we can deduce that pronounced geochemical weathering occurred in Mt. Sago, compared to Maninjau, Marapi and to a lesser extent in Singgalang-Tandikek.

A linear discriminant analysis was conducted to investigate if geochemical elements can be used to distinguish soils derived from the 4 volcanoes. Discriminant analysis using the combined 10 geochemical abundance data (SiO_2, Al_2O_3, Fe_2O_3, CaO, MgO, K_2O, SO_3, P_2O_5, Ti and Zr) of volcanic paddy-soils results in a clear distinction of soils of Mt. Sago from Maninjau, Mt. Marapi and Mt. Singgalang-Tandikek (Fig. 5). Geochemical characteristics of soils from Mt. Sago and Mt. Marapi are quite distinct, meanwhile, Singgalang-Tandikek overlaps with Maninjau. The first two canonical variates accounted for 97% variation in the data (canonical I = 72.69%, II = 24.06%, and III = 3.25%) with Eigenvalues of 4.86, 1.61 and 0.22, respectively (Table 4 and B). The significant (P < 0.0001 and 0.083) canonical correlation among soil chemical characteristics indicate the clear differentiation of soil geochemical status of each group of soils. The first canonical function is dominated by large loadings from SO_3, Fe_2O_3 and SiO_2 and a negative Zr, CaO, and Al_2O_3 loading. The second canonical function is dominated by a large loading from Ti, P_2O_5, and CaO, and with a negative loading from SO_3, Al_2O_3 and Zr. Furthermore, on the third canonical, Zr is dominated by large loading and a negative contribution from SiO_2 and Al_2O_3. Correlation between each canonical variate was observed (Table 5). The strongest positive correlations were observed between SiO_2 and both K_2O and CaO, while Zr correlated strongly with Ti, Al_2O_3, and Fe_2O_3. The strongest negative correlations were obtained between Fe_2O_3 and the oxides CaO, K_2O, SiO_2, and SO_3.

The separation of these 4 groups can also be measured by the Mahalanobis distance. The Mahalanobis distance between Sago and Singgalang-Tandikek is the largest, followed by Marapi and Maninjau indicating lithologic variation among soil parent materials and their distinction into different groups (Table 6). The geochemical signatures of Maninjau and Singgalang-Tandikek are mixed, as such the difference between the sources of these volcanic paddy soils was less marked. We assumed, they are geochemically similar and deposition of the old volcanic deposit of Maninjau caldera beneath Singgalang-Tandikek volcanic ash layers could be found.

These results are in line with Martínez-Cortizas et al. (2007) who demonstrated the use of multivariate statistical analysis to identify main pedogenesis trends in European volcanic ash soils. They further summarised that the results of the discriminant analysis indicated that, even a limited data set of chemical soil properties is sufficient to separate and characterize volcanic ash soils. Cronin et al. (1996) revealed their findings that discriminant analysis is also a useful method of discriminating tephra from the two sources in distal areas of New Zealand.

3.3. Weathering indices

The soils under humid tropical conditions are expected to be weathered intensively. The degree of weathering calculated from

Table 4
A. The canonical loadings of the measured variables of volcanic paddy soils.

Measured variables	Canonical variate		
	I	II	III
SiO_2 (%)	0.6813	0.1422	− 0.6273
Al_2O_3 (%)	− 0.2326	− 0.3662	− 0.1685
CaO (%)	− 0.5018	0.9275	0.5472
MgO (%)	− 0.0301	− 0.1136	− 0.4751
K_2O (%)	0.3611	− 0.0559	0.0220
SO_3 (%)	0.8653	− 0.7493	0.6218
P_2O_5 (ppm)	− 0.2509	0.6779	− 0.1931
Fe_2O_3 (%)	0.7670	− 0.2044	− 0.6993
Zr	− 1.1890	− 0.2590	0.8250
Ti	0.4848	1.3415	0.2208

B. Canonical details.

	Canonical variate		
	I	II	III
Eigenvalue	4.861	1.609	0.217
Percent	72.685	24.064	3.251
Cum percent	72.685	96.749	100.000
Canonical correlation	0.911	0.785	0.423
Likelihood ratio	0.054	0.315	0.821
Approx. F	11.068	5.824	1.848
Num. DF	30.000	18.000	8.000
Den. DF	194.400	134.000	68.000
Prob > F	< 0.00-01	< 0.00-01	0.083

Table 5
Relationship between canonical structures.

Parameter	SiO_2 (%)	Al_2O_3 (%)	CaO (%)	MgO (%)	K_2O (%)	SO_3 (%)	P_2O_5 (ppm)	Fe_2O_3 (%)	TiO_2	ZrO_2
Canon1	− 0.63853	0.971779	− 0.798564	− 0.716603	− 0.931528	− 0.951614	− 0.51288	0.9389959	0.9108397	0.998859
Canon2	0.7632177	0.1406542	0.5930379	0.1463079	0.356175	0.1514275	0.8229849	0.1122736	0.3845449	0.0466775
Canon3	− 0.098888	− 0.189373	0.1029611	− 0.681963	0.0734491	0.2673974	0.2442326	− 0.325087	− 0.149988	− 0.01009

SiO_2/Al_2O_3 is between 1.9 and 3.7. These values can be interpreted as moderately weathered when we compared them with the two extremes: fresh ash samples from Mt. Talang in West Sumatra (Fiantis et al., 2010) with a value of 3.6 and weathered volcanic soils from Santa Maria Island from Vanuatu, with values between 0.6 and 1.1 (Ugolini and Dahlgren, 2002).

The concentration of the two most resistant elements such as titanium (Ti) and zircon (Zr) were much higher in soils of Mt. Sago than from other volcanoes. The ZrO_2 concentration in soils from Mt. Sago was 43% higher than in Mt. Singgalang-Tandikek and 30% higher than those in Mt. Marapi and Maninjau. Positive geochemical trends exist for Zr with Al_2O_3 ($R^2 = 0.73$), TiO_2 ($R^2 = 0.69$), and Fe_2O_3 ($R^2 = 0.49$) while a negative correlation was observed with CaO ($R^2 = 0.42$), SO_3 ($R^2 = 0.55$) and K_2O ($R^2 = 0.37$). Conversely Zr weakly related to the depleted concentration of MgO and P_2O_5. Comparison of total titanium oxide (TiO_2) within studied soils showed significantly different amounts in the following order; Sago > Marapi > Maninjau > Singgalang-Tandikek.

When analysing other weathering indices, their mean values showed a moderate to almost optimum weathering stage. Paddy soils of Mt. Sago showed the lowest mean values for Ruxton (1.88) and desilication index (1.15), Ti/Zr (20.46) and CTR (0.02) followed by soils of Maninjau, Marapi and Singgalang-Tandikek as presented in Fig. 6. Ruxton and Desilication indices indicated the following order from largest to smallest weathering intensity: Sago > Maninjau > Marapi > Singgalang-Tandikek.

This weathering pattern is also reflected in the ratio of base loss and Ba/Sr leaching (Fig. 7). Soils of Mt. Sago exhibited significant loss of more base cations and barium over strontium compared to other soils. The base loss index in Maninjau, Marapi and Mt. Singgalang-Tandikek were relatively similar while the ratio of Ba/Sr leaching in Maninjau was two times higher than in Marapi and Singgalang-Tandikek. The depleted amount of basic cations and accrual of Al_2O_3, Fe_2O_3, TiO_2 and ZrO_2 during soil the weathering process was clearly observable in the studied soils. The parent material of soils in Mt. Sago, presumably, is older than those in Marapi, Maninjau, and Singgalang-Tandikek. As

Table 6
Pairwise squared distance between four groups of volcanic paddy-soils.

Rotation	Sago	2_Singgalang-Tandikek	Marapi	Maninjau
Sago	–	7.26	5.57	4.84
Singgalang-Tandikek	7.26	–	4.15	3.69
Marapi	5.57	4.15	–	5.01
Maninjau	4.84	3.69	5.01	–

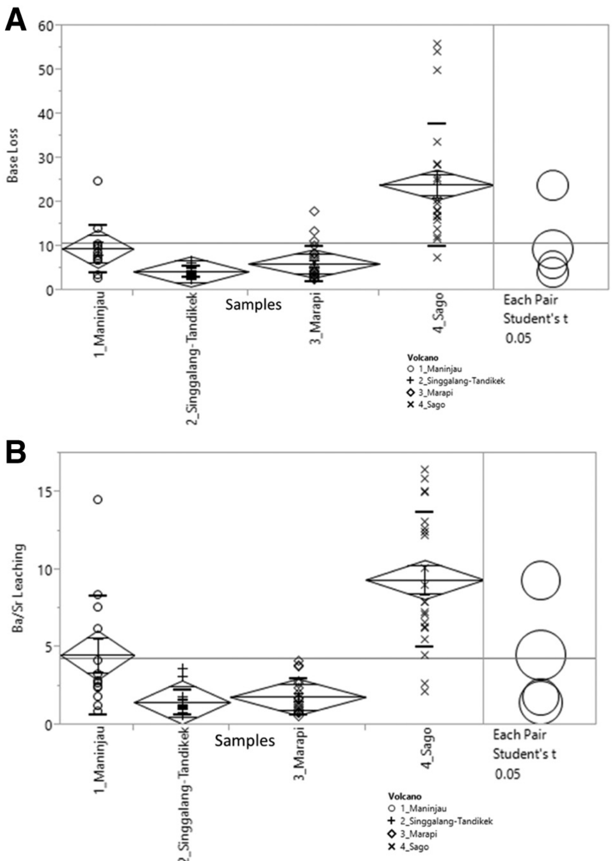

Fig. 6. Oneway analysis of weathering indices by volcano.

there is no age data available, we can assume that the age of Mt. Sago tephra is somewhat older than that of Maninjau which was found to be 50 ka for the youngest volcanic deposit (Nishimura, 1980) and also based on the absence of pumiceous tuff deposit of Maninjau overlying tephra of Mt. Sago (Mohr, 1944).

3.4. Soil carbon and its fractions

As opposed to geochemical signatures, there is no trend in soil total C across soils from the 4 volcanoes. This is because the C content of these soils are quite high (> 2%) and all soils have been used for paddy cultivation. However, FTIR analysis of the soils reveals some interesting trends. The mid-infrared reflectance spectra for typical soils of the 4 mountains are shown in Fig. 8. The peak near 2930 cm^{-1} corresponds to stretching vibrations of the C—H bonds of aliphatic carbon, while the peak at 1620 cm^{-1} is associated with aromatic carbon with C=C bond. Spectra analysis using the area under the absorbance curve showed that organic matter is mainly represented by bands at 2930 cm^{-1}, 1620 cm^{-1}, 1530 cm^{-1} and 1159 cm^{-1}, ranging up to 71, 26, 2 and 1% respectively as shown in Fig. 9. Most organic matter is found at the 2930 cm^{-1} peak, (and strongly reflects increasing total C) which is associated with aliphatic (C—H) and considered here as a labile carbon fraction (Demyan et al., 2012 and Margenot et al., 2015).

Soils of Mt. Sago, which are most weathered, have a high total C content (mean 3.1%) but the organic matter is strongly represented by aliphatic C—H compounds (peak 2930 cm^{-1}). Mt. Sago soils have the highest relative abundance of aliphatic SOM compared to soils of Maninjau, Singgalang-Tandikek, and Marapi with the average abundance of 77, 71, 71 and 64%, respectively. On the other hand, soils of Mt. Marapi, which are relatively the least weathered and have the lowest C content (mean 2.4%), exhibited higher concentrations of the more stable aromatic C=C fraction (peak 1620 cm^{-1}) and significantly

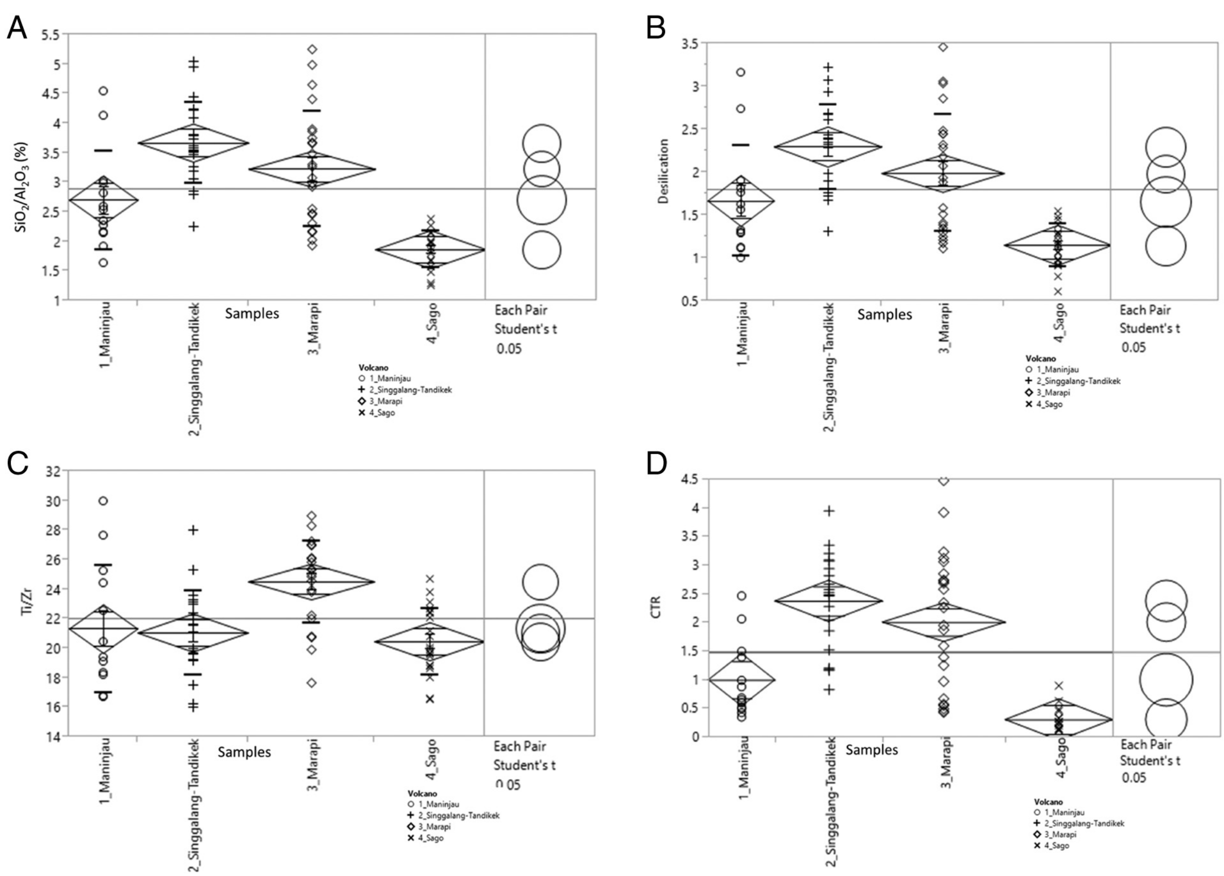

Fig. 7. Oneway analysis of base loss and Ba/Sr leaching by volcano.

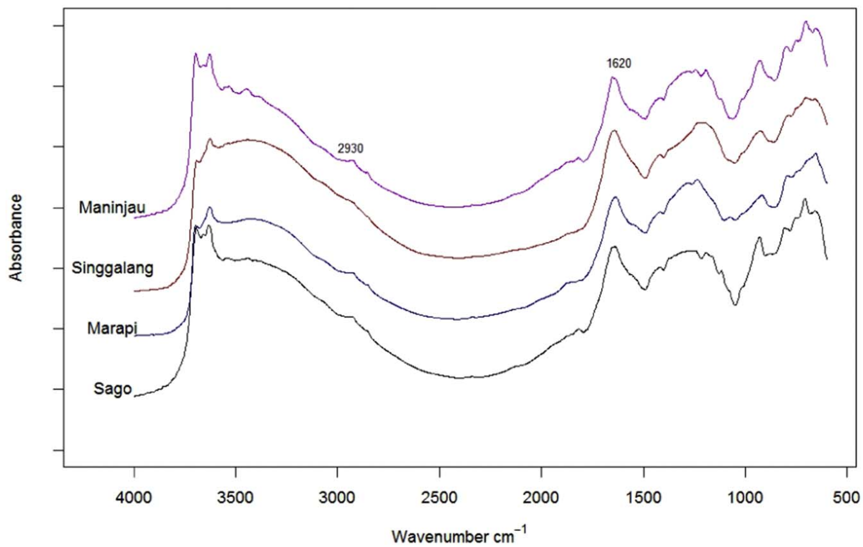

Fig. 8. Absorbance spectra of volcanic-paddy soils of West Sumatra.

different to those present in Singgalang-Tandikek, Maninjau and Sago averaging at of 33, 26, 25 and 19%, respectively. The other two carbon fractions (including C—O functional groups) were only minor between 1 and 2% in all soils. The ratio of stable (aromatic) to labile (aliphatic) determined by 1620/2930 cm^{-1} as proposed by Demyan et al. (2012), showed that the stable C decreases with increasing C content (Fig. 10). This result suggests that there is a limit of the soils to hold the more stable aromatic C as demonstrated in Mt. Marapi. Soils at Mt. Sago and Singgalang-Tandikek which have a concentration > 3% are mostly composed of labile organic matter. Soils with total C < 2% tend to be dominated by aromatic fractions, while soils > 2% C are dominated by the more labile aliphatic fractions.

A positive relationship was observed between the absorbance at peak 1620 cm^{-1} and SiO_2 ($r = 0.46$) which suggested a higher capacity of SiO_2 to retain or specifically adsorb the aromatic carbon fraction in soil, as such preventing them from biodegradation. This finding is in agreement with Pisani et al. (2014) who showed that volcanic soils of Costa Rica accumulated 73% aliphatic compounds in the SOM, which highly correlated with the allophane content and was found more prevalent in grassland than forest. Typical minerals associated with SiO_2 in volcanic soils are allophane and imogolite, both of which have non-crystalline and para-crystalline structures, respectively (Dahlgren et al., 2004).

It is also interesting to note on Fig. 8 that soils from Maninjau and Sago displayed distinct kaolinite signature of OH-stretching region of 3563 cm^{-1} which implied that they are weathered further than Singgalang and Marapi which showed broader peaks at 3698 and 3622 cm^{-1} (Ryan et al., 2016). This FTIR signature is consistent with

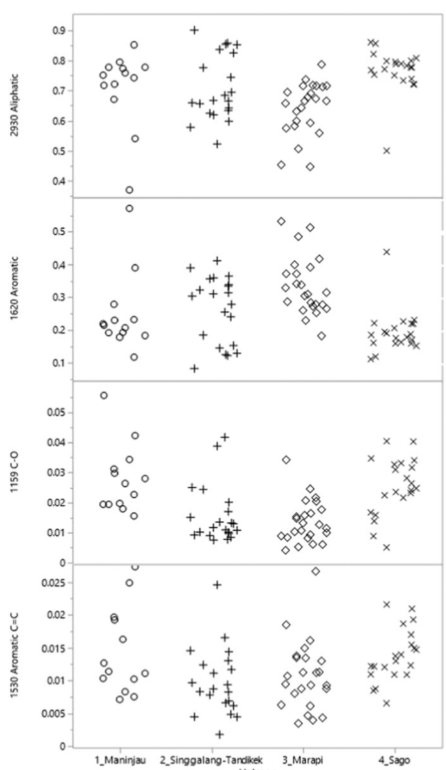

Samples	Number	Mean	Std Error	Lower 95%	Upper 95%
Maninjau	13	0.71	0.027	0.66	0.77
Singgalang-Tandikek	21	0.71	0.021	0.69	0.75
Marapi	24	0.64	0.020	0.60	0.68
Sago	21	0.77	0.021	0.73	0.81

Samples	Number	Mean	Std Error	Lower 95%	Upper 95%
Maninjau	13	0.25	0.026	0.20	0.30
Singgalang-Tandikek	21	0.26	0.020	0.22	0.30
Marapi	24	0.33	0.019	0.30	0.37
Sago	21	0.19	0.020	0.15	0.23

Samples	Number	Mean	Std Error	Lower 95%	Upper 95%
Maninjau	13	0.03	0.002	0.02	0.03
Singgalang-Tandikek	21	0.016	0.002	0.01	0.02
Marapi	24	0.013	0.002	0.01	0.02
Sago	21	0.025	0.002	0.02	0.03

Samples	Number	Mean	Std Dev	Lower 95%	Upper 95%
Maninjau	13	0.01	0.007	0.01	0.02
Singgalang-Tandikek	21	0.01	0.005	0.01	0.01
Marapi	24	0.01	0.005	0.01	0.01
Sago	21	0.01	0.004	0.01	0.02

Fig. 9. Visualization of the entire soil organic matter using scatter plot matrix and their statistical data.

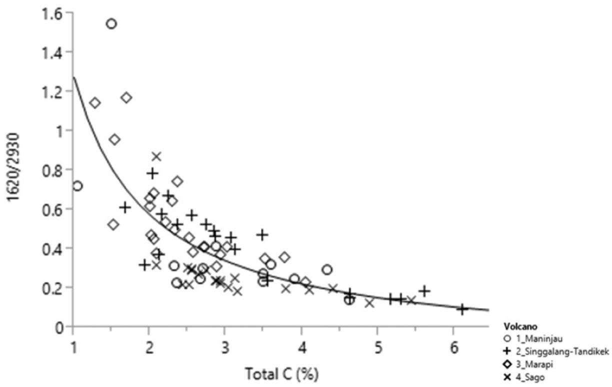

Fig. 10. Bivariate fit of 1620/2930 by total C (%).

the desilication index presented in the previous section.

4. Conclusions

This study showed although volcanic soils have been used for many years as paddy soils in West Sumatra, they still retain their geochemical signatures. In addition to conventional soil physical and chemical analysis, geochemical elemental concentration and weathering indices can be rapidly measured using a portable X-ray fluorescent spectrometer. The geochemical parameters revealed that soils of Mt. Sago demonstrated different chemical characteristics compared to those from Mts. Marapi, Singgalang-Tandikek, and Maninjau. We established that soils of Mt. Sago are more weathered as indicated by the high amount of resistant oxides of Ti, Zr, Al and Fe, low weathering indices, and the larger loss of base cations compared to other groups of volcanic soils.

Using FTIR, soil carbon fractions from the soils can be quantified. Aliphatic fractions were the dominant carbon components and considered as labile with abundances between 64 and 77%. Increasing C content trended with increases in the labile fractions and decreases in the more stable aromatic fractions. The data from this study suggests a saturation limit of about 2% C for the more stable aromatic fraction.

Future studies will consider the field application of a portable XRF and mid-infrared spectrometer for rapid acquisition of soil's geochemical properties for pedogenesis study (Hartemink and Minasny, 2014).

Acknowledgements

The work leading to these results has received funding from Universitas Andalas under grant agreement no. 68/UN.16/HKRGB/LPPM/2016 to first two authors. A sabbatical grant from Universitas Andalas to Sydney University was granted to the first author. The support from Sydney South East Asia Centre (no. 06062016) enabled this work to be carried out at the Faculty of Agriculture and Environment, The University of Sydney.

Appendix A. Supplementary data

Supplementary data associated with this article can be found in the online version, at doi: http://dx.doi.org/10.1016/j.geodrs.2017.04.004. These data include the Google map of the most important areas described in this article.

References

Aimrun, W., Amin, M.S., Eltaib, S., 2004. Effective porosity of paddy soils as an estimation of its saturated hydraulic conductivity. Geoderma 121, 197–203.

Alloway, B.V., Pribadi, A., Westgate, J.A., Bird, M., Fifield, L.K., Hogg, A., Smith, I., 2004. Correspondence between glass-FT and ^{14}C ages of silicic pyroclastic flow deposits sourced from Maninjau caldera, west-central Sumatra. Earth Planet. Sci. Lett. 227, 121–133.

Anda, M., 2012. Cation imbalance and heavy metal content of seven Indonesian soils as affected by elemental compositions of parent rocks. Geoderma 189–190, 388–396.

Anda, M., Suparto, Sukarman, 2016. Characteristics of pristine volcanic materials: beneficial and harmful effects and their management for restoration of agroecosystem. Sci. Total Environ. 543, 480–492.

Bétard, F., 2012. Spatial variation of soil weathering processes in a tropical mountain environment: the Baturité massif and its pediment (Ceará, NE Brazil). Catena 93, 18–28.

Blakemore, L.C., Searle, P.L., Daly, B.K., 1987. Methods for chemical analysis of soils. In: NZ Bureau Scientific Report 80. Bur, Lower Hutt, NZ, NZ Soil (43 p).

Buggle, B., Glaser, B., Hambach, U., Gerasimenko, N., Markovic, S., 2011. An evaluation of geochemical weathering indices in loess – paleosols studies. Quat. Int. 240, 12–21.

Campbell, S., Malone, B., Minasny, B., Nelson, M., Fajardo, M., 2016. Spectroscopy: Functions for Visible and Near Infrared Data Manipulation. (URL:https://github.com/Soilsecuritylab/spectroscopy_package).

Cronin, S.J., Wallace, R.C., Neall, V.E., 1996. Sourcing and identifying andesitic tephras using major oxide titanomagnetite and hornblende chemistry, Egmont volcano and Tongariro Volcanic Centre, New Zealand. Bull. Volcanol. 58, 33–40.

Dahlgren, R., Saigusa, M., Ugolini, F.G., 2004. The nature, properties and management of volcanic soils. Adv. Agron. 82, 113–182.

Demyan, M.S., Rasche, F., Schulz, E., Breulmann, M., Muller, T., Cadish, G., 2012. Use of specific peaks obtained by diffuse reflectance Fourier transform mid-infrared spectroscopy to study the composition of organic matter in a Haplic Chernozem. Eur. J. Soil Sci. 63, 189–199.

Drew, L.J., Grunsky, E.C., Sutphin, D.M., Woodruff, L.G., 2010. Multivariate analysis of the geochemistry and mineralogy of soils along two continental-scale transects in North America. Sci. Total Environ. 409, 218–227.

Fauzi, A.I., Stoops, G., 2004. Reconstruction of a toposequence on volcanic material in the Honje Mountains, Ujung Kulon Peninsula, West Java. Catena 56, 45–66.

Fiantis, D., 2000. Colloid-Surface Characteristics and Amelioration Problems of Some Volcanic Soils in West Sumatra, Indonesia. PhD thesis Universiti Putra Malaysia, Serdang, Selangor, Malaysia.

Fiantis, D., Van Ranst, E., Shamshuddin, J., Fauziah, C.I., Zauyah, S., 2002. Effect of calcium silicate and superphosphate application on surface charge properties of volcanic soils from west Sumatra, Indonesia. Commun. Soil Sci. Plant Anal. 33, 1887–1900.

Fiantis, D., Nelson, M., Shamshuddin, J., Goh, T.B., Van Ranst, E., 2010. Determination of the weathering indices and trace elements content of new volcanic ash deposits from Mt. Talang (West Sumatra) Indonesia. Eurasian Soil Sci. Vol. 43 (13) (1487–1485).

Fiantis, D., Nelson, M., Shamshuddin, J., Goh, T.B., van Ranst, E., 2011. Changes in the chemical and mineralogical properties of Mt. Talang volcanic ash in West Sumatra during the initial weathering phase. Commun. Soil Sci. Plant Anal. 42, 569–585.

Hartemink, A.E., Minasny, B., 2014. Towards digital soil morphometrics. Geoderma 230, 305–317.

Hazelton, P., Murphy, B., 2007. Interpreting Soil Test Results, What do All the Numbers Mean. CSIRO Publishing, Collingwood, Vic 3066 Australia (152 p. ISBN 978 0 64309 225 9).

Hochstein, M.P., Sudarman, S., 1993. Geothermal resources of Sumatra. Geothermics 22, 181–200.

Kastowo, Leo, Gafoer, G.W., Amin, T.C., S., 1996. Geological Map of Padang Quadrangle, Sumatra. Geological Research and Development Centre. Scale 1:250.000 With Explanation. Bandung.

Kölbl, A., Schad, P., Jahn, R., Amelung, W., Bannert, A., Cao, Z.H., Fiedler, S., Lehndorff, E., Müller-Niggemann, C., Schloter, M., Schwark, L., Vogelsang, V., Wissing, L., Kögel-Knabner, I., 2014. Accelerated soil formation due to paddy management on marshlands (Zhejiang Province), China. Geoderma 228, 67–89.

Kontgis, C., Schneider, A., Ozdogan, M., 2015. Mapping rice paddy extent and intensification in the Vietnamese Mekong River Delta with dense time stacks of Landsat data. Remote Sens. Environ. 169, 255–269.

Kopittke, P.M., Menzies, N.W., 2007. A review of the use of the basic cation saturation ratio and the “ideal” soil. Soil Sci. Soc. Am. J. 71, 259–265.

Kronberg, G.I., Nesbitt, H.W., 1981. Quantification of weathering of soil chemistry and soil fertility. J. Soil Sci. 32, 453–459.

Leo, G.W., Hedge, C.E., Marvin, R.F., 1980. Geochemistry, strontium isotope data, and potassium–argon ages of the andesite–rhyolite association in the Padang area, West Sumatra. J. Volcanol. Geotherm. Res. 7, 139–156.

Margenot, A.J., Calderon, F.J., Bowles, T.M., Parikh, S.J., Jackson, L.E., 2015. Soil organic matter functional group composition in relation to organic carbon, nitrogen, and phosphorus fractions in organically managed tomato field. Soil Sci. Soc. Am. J. 79, 772–782.

Martin, M., Stanchi, S., Jakeer Hossain, K.M., Imamul Huq, S.M., Barberis, E., 2015. Potential phosphorus and arsenic mobilization from Bangladesh soils by particle dispersion. Sci. Total Environ. 536, 973–980.

Martínez-Cortizas, A., Nóvoa, J.C., Pontevedra, X., Taboada, T., García-Rodeja, E., Buurman, P., 2007. Multivariate statistical analysis of chemical properties of European volcanic soils. In: Arnalds, O. (Ed.), Soils of Volcanic Regions in Europe. Springer, Berlin Heidelberg New York, pp. 387–400.

Mohr, E.C.J., 1938. The relation between soil and population density in the Netherlands Indies. In: Comptes Rendus du Congres International du Geographie. Vol. 103. Tome Deuxieme, Amsterdam, pp. 478–493.

Mohr, E.G.J., 1944. The Soils of Equatorial Region With Special Reference to the Netherlands East Indies. Edward Brother, Inc., Ann Arbor Michigan USA (766 p).

Muslim, A.R., 2015. Big Eruption of Mt. Marapi in West Sumatra and Three Times of Earthquake Last Night. http://news.liputan6.com/read/2366076/gunung-marapi-di-sumbar-meletus-besar-semalam-dan-3-kali-gempa (In Indonesian).

Nesbitt, H.W., Markovics, G., Price, R., 1980. Chemical processes affecting alkalis and alkaline earths during continental weathering. Geochim. Cosmochim. Acta 44,

1659–1666.
Nguyen, Y.T.B., Araki, Y., Ouk, M., 2013. Water availability, management practices and grain yield for deep water rice in Northwest Cambodia. Field Crop Res. 152, 44–56.
Nishimura, S., 1980. Reexamination of the fission-track ages of volcanic ashes and ignimbrites in Sumatra. In: Nishimura, S. (Ed.), Physical Geology of Indonesian Island Arcs. Kyoto University, pp. 148–153.
Parelho, C., Rodrigues, A.S., Cruz, J.V., Garcia, P., 2014. Linking trace metals and agricultural land use in volcanic soils — a multivariate approach. Sci. Total Environ. 496, 241–247.
Pisani, O., Hills, K.M., Courtier-Murias, D., Haddix, M.L., Paul, E.A., Conant, R.T., Simpson, A.J., Arhonditsis, G.B., Simpson, M.J., 2014. Accumulation of aliphatic compounds in soil with increasing mean annual temperature. Org. Geochem. 76, 118–127.
Prakongkep, N., Suddhiprakarn, A., Kheoruenromne, I., Smirk, M., Gilkes, R.J., 2008. The geochemistry of Thai paddy soils. Geoderma 144, 310–324.
Rinklebe, J., Shaheen, S.M., Yu, K., 2016. Release of As, Ba, Cd, Cu, Pb, and Sr under pre-definite redox conditions in different rice paddy soils originating from the U.S.A. and Asia. Geoderma 270, 21–32.
Ruxton, B.P., 1968. Measure of the degree of chemical weathering of rocks. J. Geol. 76, 518–527.
Ryan, P.C., Huertas, F.J., Hobbs, F.W.C., Pincus, L.N., 2016. Kaolinite and halloysite derived from sequential transformation of pedogenic smectite and kaolinite-smectite in a 120 ka tropical soil chronosequence. Clay Clay Miner. 64 (5), 639–667.
Silitonga, P.H., Kastowo, 1995. Geological Map of Solok Quadrangle, Sumatra. Geological Research and Development Centre, Bandung.
Singh, L.P., Parkash, B., Singhvi, A.K., 1998. Evolution of the lower gangetic plain landforms and soils in West Bengal, India. Catena 33, 75–104.
Small, C., Naumann, T., 2001. The global distribution of human population and recent volcanism. Global Environ. Change B. Environ. Hazard 3 (3), 93–109.
Smyth, H.R., Crowley, Q.G., Hall, R., Kinny, P.D., Hamilton, P.J., Schmidt, D.N., 2011. A Toba-scale eruption in the Early Miocene: the Semilir eruption, East Java, Indonesia. Lithos 126, 198–211.
Soil Survey Staff, 2014. Keys to Soil Taxonomy. United States Department of Agriculture Natural Resources Conservation Service, Washington DC (20250-9419 USA).
Stockmann, U., Cattle, S.R., Minasny, B., McBratney, A.B., 2016. Utilizing portable X-ray fluorescence spectrometry for in-field investigation of pedogenesis. Catena 139, 220–231.
Tan, K.H., 2005. Soil Sampling, Preparation, and Analysis. Taylor & Francis Group, Boca Raton FL USA (623 p).
Ugolini, F.C., Dahlgren, R.A., 2002. Soil development in volcanic ash. Global Environ. Res. 6, 69–81.
Van Bemmelen, R.W., 1949. The Geology of Indonesia. Vol. I A Martinus Nijhoff, The Hague (732 p).
Van Ranst, E., Utami, S.R., Verdoodt, A., Qafoku, N.P., 2008. Mineralogy of a perudic andosol in central Java, Indonesia. Geoderma 144, 379–386.
Ward, P.A., Carter, B.J., Weaver, B., 1993. Volcanic ashes: time markers in soil parent materials of the Southern Plains. Soil Sci. Soc. Am. J. 57, 453–460.
Webster, R., 1977. Quantitative and Numerical Methods in Soil Classification and Survey. Clarendon Press, Oxford University Press, London0-19-854512-6 (269 p).
Winkler, P., Kaiser, K., Kölbl, A., Kühn, T., Schad, P., Urbanski, L., Fiedler, S., Lehndorff, E., Kalbitz, K., Utami, S.R., Cao, Z., Zhang, G., Jahn, R., Kögel-Knabner, I., 2016. Response of vertisols, andosols, and alisols to paddy management. Geoderma 261, 23–35.